Resident PW1(+) Progenitor Cells Participate in Vascular Remodeling During Pulmonary Arterial Hypertension

France Dierick, Tiphaine Héry, Bénédicte Hoareau, Nathalie Mougenot, Virginie Monceau, Caroline Claude, Mihaela Crisan, Vanessa Besson, Peter Dorfmüller, Gilles Marodon, et al.

Resident PW1^{+} progenitor cells participate in vascular remodeling during pulmonary arterial hypertension

Short title: Resident PW1 Progenitor Cells participate in PH

Authors and Affiliations

France Dierick[1], Tiphaine Héry[1], Bénédicte Hoareau-Coudert[2], Nathalie Mougenot[3], Virginie Monceau[1], Caroline Claude[1], Mihaela Crisan[4], Vanessa Besson[1], Peter Dorfmüller[5,6], Gilles Marodon[7], Elie Fadel[5,8], Marc Humbert[5,9,10], Elisa Yaniz-Galende[1], Jean-Sébastien Hulot[1], Giovanna Marazzi[1], David Sassoon[1], Florent Soubrier[1] and Sophie Nadaud[1].

1. Sorbonne Universités, UPMC Univ Paris 06, INSERM, Institute of Cardiometabolism and Nutrition, UMR_S 1166-ICAN, F-75005 Paris, France
2. Sorbonne Universités, UPMC Univ Paris 06, UMS-030 CyPS, F-75005 Paris, France
3. Sorbonne Universités, UPMC Univ Paris 06, PECMV UMS28, F-75005 Paris, France
4. Erasmus MC Stem Cell Institute, Rotterdam, Pays-Bas
5. Univ. Paris-Sud, Université Paris Saclay, INSERM UMR-S 999, Labex LERMIT, Le Plessis-Robinson, France
6. Service d'Anatomie Pathologique, Centre Chirurgical Marie Lannelongue, Le Plessis Robinson, France
7. Sorbonne Universités, UPMC Univ Paris 06, INSERM, CNRS, CR7, Centre d'Immunologie et des Maladies Infectieuses (CIMI), IU1135, ERL 8255, F-75013 Paris, France.
8. Service de Chirurgie Thoracique et Vasculaire, Centre Chirurgical Marie Lannelongue, Le Plessis-Robinson, France
9. Univ. Paris-Sud, Université Paris Saclay, Le Kremlin-Bicêtre, France
10. Assistance Publique Hôpitaux de Paris, Service de Pneumologie, Centre de Référence de l'Hypertension Pulmonaire Sévère, Hôpital Bicêtre, Le Kremlin Bicêtre, France

Correspondence should be addressed to Sophie Nadaud
Dr Sophie Nadaud, PhD
UMR_S 1166 ICAN
Faculté de Médecine Pitié-Salpêtrière, 3ème étage - 91 Boulevard de l'hôpital - 75013 Paris
Telephone number +33 140779927
E-mail address: sophie.nadaud@upmc.fr

Total word count of the manuscript: 7354

ABSTRACT

Rationale - Pulmonary arterial hypertension (PAH) is characterized by vascular remodeling and neomuscularization. $PW1^+$ progenitor cells can differentiate into smooth muscle cells (SMC) *in vitro*.

Objective – To determine the role of pulmonary $PW1^+$ progenitor cells in vascular remodeling characteristic of PAH.

Methods and Results - We investigated their contribution during chronic hypoxia (CH)-induced vascular remodeling in *Pw1*$^{nLacZ+/-}$ mouse expressing β-galactosidase in $PW1^+$ cells and in differentiated cells derived from $PW1^+$ cells. $PW1^+$ progenitor cells are present in the perivascular zone in rodent and human control lungs. Using progenitor markers, three distinct myogenic $PW1^+$ cell populations were isolated from the mouse lung of which two were significantly increased after 4 days of CH. The number of proliferating pulmonary $PW1^+$ cells and the proportion of β-gal^+ vascular SMC were increased, indicating a recruitment of $PW1^+$ cells and their differentiation into vascular SMC during early CH-induced neomuscularization. CXCR4 inhibition using AMD3100 prevented $PW1^+$ cells differentiation into SMC but did not inhibit their proliferation. Bone marrow transplantation experiments showed that the newly formed β-gal^+ SMC were not derived from circulating bone marrow-derived $PW1^+$ progenitor cells, confirming a resident origin of the recruited $PW1^+$ cells. The number of pulmonary $PW1^+$ cells was also increased in rats after monocrotaline (MCT) injection. In lung from pulmonary arterial hypertension patients, PW1-expressing cells were observed in large numbers in remodeled vascular structures.

Conclusions - These results demonstrate the existence of a novel population of resident SMC progenitor cells expressing PW1 and participating in PH-associated vascular remodeling.

Keywords: vascular progenitor cell, smooth muscle cell, neomuscularization, pulmonary arterial hypertension

Abbreviations:

PAH, Pulmonary Arterial Hypertension; PH, Pulmonary Hypertension; CH, chronic hypoxia; MCT, monocrotaline; SMC, smooth muscle cell; α-SMA, alpha-smooth muscle actin; CNN1, calponin; SM-MHC, smooth muscle myosin heavy chain; EC, endothelial cell; RVSP, right ventricular systolic pressure; SDF-1, Stromal-derived factor-1; MIF, Macrophage migration inhibitory factor; BM, bone marrow.

INTRODUCTION

Pulmonary arterial hypertension (PAH), a rare and severe disease with no curative options, is characterized by a sustained increase in pulmonary vascular resistance leading to right heart failure and death[1]. Histologically, PAH is associated with neomuscularization of small pulmonary vessels, medial hypertrophy, neointima formation, endothelial proliferation, excessive extracellular matrix deposition and recruitment of inflammatory cells in the vascular wall [2–4]. To date, the cellular origin of neomuscularization and medial hypertrophy remain unknown. It was proposed that new smooth muscle cells (SMC) are derived from resident SMC that re-enter a proliferative state [5] or from pericytes [6,7] and/or from endothelial cells (EC) that adopt a smooth muscle fate [8]. Recent studies suggest that SMC originate from the proliferation and differentiation of either resident as well as circulating bone marrow (BM)-derived progenitor cells [9]. Indeed, various types of resident SMC progenitor cells have been identified in numerous adult organs, including the lung. They are located in the vessel or in the perivascular zone and express several stem cells markers including Sca-1, c-kit, PDFGR-α or CD34 or mesenchymal stem cells markers [10,11]. In addition, perivascular cells identified by these same markers and expressing CD146, NG2 and PDGFR-β were also recognized as SMC progenitor cells [12].

Recently, a population of interstitial progenitor cells was identified in mouse skeletal muscle based on their expression of the PW1 protein [13] which are capable of giving rise to smooth and skeletal muscle as well as adipocytes in culture [14,15]. These PW1-expressing cells were found in multiple adult tissues including skin, gut, BM and the central nervous system [14]. *Pw1* gene encodes a zinc-finger protein that has been shown to regulate cell cycle and cell stress responses due to inflammation [16] and p53 [17]. In addition, PW1 mediates β-catenin stability in the Wnt signalling pathway [18]. PW1 has also been shown to function as a transcription factor with a DNA-binding motif regulating a large array of genes involved in metabolic homeostasis [19]. Moreover, PW1 expression is required for the myogenic and migratory capacities of both mouse and human mesoangioblasts, reinforcing the relevance of PW1 to identify competent mesoangioblasts prior to their use in stem cell-mediated therapeutic applications[20].

Given the distribution of PW1 expression in a wide array of adult somatic stem cells and the role of PW1 in cell stress responses, we investigated whether $PW1^{+}$ progenitor cells present in lung tissue are recruited to proliferate and differentiate into SMCs during vascular remodeling during chronic hypoxia (CH)-induced PH. To address this hypothesis, we used a PW1-reporter transgenic mouse, $PW1^{nLacZ/+}$, that expresses the nuclear β-galactosidase within the *Pw1* gene context [14]. These mice carry the β-galactosidase coding sequence (β-gal) driven under the control of *Pw1* and due to the high level and stability of the reporter gene product [21], we can identify cells recently derived from reporter expressing progenitor cells. In this study, we used this reporter mouse to examine the role of the $PW1^{+}$ progenitor cells in vascular remodeling during CH. We identified two resident $PW1^{+}$ progenitor cell populations located in the lung parenchyma and in perivascular zones of small pulmonary vessels, which show an early recruitment and a potential to differentiate into SMCs during CH. Our results strongly suggest that new SMC derive from resident $PW1^{+}$ progenitor cells recruited during early CH.

METHODS

Detailed methods are provided in the online data supplement.

Pw1IRESnLacZ transgenic mice (*Pw1*$^{nlacZ/+}$) bear a nuclear operon lactose gene expressed under the control of the *Pw1* gene locus[18]. Mice (littermates of 6-8 weeks) were exposed to room air (normoxia) or chronic normobaric hypoxia (10% O_2) for 4 or 28 days. Fluorescence-activated cell sorting (FACS) was used to isolate the pulmonary PW1$^+$ cell populations based on their β-gal activity and a combination of progenitor markers. Lethally irradiated C57BL6/J mice were reconstituted with BM cells of age and sex-matched GFP$^+$/β-gal$^+$ (H2B-GFPx*Pw1*$^{nLacz/+}$) mice and exposed, after 9 months, to Normoxia (N) or CH for 4 days (CH 4d).

RESULTS

Mouse pulmonary PW1$^+$ cells are present in perivascular and parenchymal zones, express progenitor and pericyte markers and differentiate into SMC.

PW1 expression was found to identify adult stem and progenitor cells in multiple organs[14,15,20] although previous studies did not report on expression in the lung. PW1 protein expression was detected by immunofluorescence in cells located in parenchymal and perivascular spaces, near small non-muscularized and muscularized vessels (Figure 1A and 1B). We characterized these progenitor cells from PW1-reporter mice after FACS purification based on β-galactosidase activity [14]. Among the CD45$^-$ cells (Online Figure I), we observed the highest levels of reporter activity in 3 populations: the PW1$^+$/CD34$^+$/c-kit$^+$ cells, the PW1$^+$/CD34$^+$/c-kit$^-$/PDGFR-α$^+$ cells and the PW1$^+$/CD34$^-$/CD146$^+$ cells (Figure 1C). These results were confirmed by direct PW1 immunostaining for each purified population, which showed a high proportion of PW1-expressing cells (74 ± 0.6% for PW1$^+$/CD34$^+$/c-kit$^+$ cells; 92 ± 2.4% for PW1$^+$/CD34$^+$/c-kit$^-$/PDGFR-α$^+$ cells; 86 ± 6.1% for PW1$^+$/CD34$^-$/CD146$^+$ cells, n=4) (Figure 1D). The PW1$^+$/CD34$^-$/CD146$^+$ cells were positive for pericyte markers NG2 (84 ± 7.3%, n=2) and PDGFR-β (86 ± 5.3%, n=2) and negative for CD31 (data not shown) (Online Figure II). Immunofluorescence studies confirmed that, in the lung, PW1 expression partially colocalized with progenitor markers CD146, c-kit and PDGFR-α (Figure 1E).

To investigate *in vitro* the potentials of these progenitor cells for differentiation in SMC, freshly sorted PW1$^+$ cell populations were studied for SMC markers either upon isolation or after cell culture and differentiation induction. Freshly sorted PW1$^+$ cells were negative for the SMC markers α-SMA and SM-MHC (Figure 2A). In culture, PW1$^+$/CD34$^+$/c-kit$^-$/PDGFR-α$^+$ cells spontaneously differentiated into α-SMA$^+$ cells (71 ± 2.3%, n=3) and into terminally differentiated α-SMA$^+$/SM-MHC$^+$ SMCs (26 ± 7%, n=3). In contrast, the PW1$^+$/CD34$^-$/CD146$^+$ and PW1$^+$/CD34$^+$/c-kit$^+$ populations differentiated into α-SMA$^+$ (66 ± 4.2% and 90.5 ± 0.7%, respectively) and α-SMA$^+$/SM-MHC$^+$ cells (4.5 ± 6.3% and 14 ± 4%, respectively) only upon induction with TGF-β_1 and PDGF-BB (n=3) (Figure 2B). Following differentiation, 50% of the cells lost β-gal expression after ~5 days of culture confirming a

downregulation of PW1 expression in differentiated cells (data not shown). Hence, all three $PW1^+$ cell populations showed robust SMC differentiation capacity *in vitro*.

The PW1-reporter mice were also used to follow the differentiation of $PW1^+$ cells *in vivo*. Because of the long half-life of β-galactosidase protein [21], this transgenic strain allows for the detection of differentiated cells recently derived from β-gal^+/$PW1^+$ progenitor cells. Indeed, in small pulmonary vessels under normoxic conditions, we observed many SMC co-expressing β-galactosidase and α-SMA (35 ± 2.2% of β-gal^+/α-SMA^+ cells), calponin (44 ± 3% of β-gal^+/$CNN1^+$ cells) or SM-MHC (54 ± 7.3% β-gal^+/SM-MHC^+ cells) but we observed very few SMC expressing PW1 (less than 7% of SMC) (Figure 2C, 5C and Online Figure III). Taken together, these results show that the lung contains three populations of $PW1^+$ SMC progenitor cells and suggest that, *in vivo*, numerous SMC are derived from $PW1^+$ progenitor cells.

We also tested the capacity of lung $PW1^+$ progenitor cells to differentiate into other vascular cells (endothelial cells) or other muscle cells (skeletal muscle cells). After *in vitro* differentiation induction, cells were labeled with anti-vWF (endothelial marker) or anti-skeletal myosin heavy chain (MF20, skeletal muscle marker) antibodies. For all 3 $PW1^+$ cell populations, we did not observe any differentiation neither in EC nor in skeletal muscle cells (Online Figures IV-A and V). Moreover, whereas most of the vascular β-gal^+ cells are SMC cells in $Pw1^{nlacZ/+}$ mice lungs, we found only rarely vascular endothelial cells expressing β-gal (Online Figure IV-B). These *in vivo* and *in vitro* data indicate that pulmonary $PW1^+$ progenitor cells do not differentiate into endothelial or skeletal muscle cells.

Pulmonary $PW1^+$ progenitor cells are recruited in two rodent PH experimental models

We next aimed to determine whether $PW1^+$ progenitor cells are recruited during CH and participate in pulmonary vascular remodeling by differentiating into SMC. Pulmonary $PW1^+$ cell populations were analyzed by FACS after 4 days of N or CH. We observed a significant increase in the number of $PW1^+$/$CD34^+$/c-kit^+ and $PW1^+$/$CD34^+$/c-kit^-/PDGFR-α^+ cells after 4 days of CH (0.4 ± 0.3% in N vs 2.5 ± 1.3% in CH, $p<0.001$ and 0.4 ± 0.2% in N vs 0.89 ± 0.27% in CH, $p<0.001$ respectively) (Figure 3A). These results were confirmed by immunofluorescence experiments showing that the number of pulmonary $PW1^+$ cells was also significantly increased after 4 days of CH (3.5 fold, $p<0.05$) (Figure 3B). Double-labeled immunofluorescent staining of lung tissues from BrdU-injected mice revealed a significant increase in the number of proliferating $BrdU^+$ PW1-expressing cells in the lung parenchyma (0.96 ± 0.4% vs 3.16 ± 0.66%, $p<0.01$) (Figure 3C). We studied the recruitment of $PW1^+$ progenitor cells in the MCT-injected rat a different, more severe and inflammatory rodent PH model (Online Figure VI). The number of lung parenchymal $PW1^+$ cells (Figure 4A) was found to be significantly increased in MCT-treated rats as compared with control animals (11.7 ± 3.1% vs 20 ± 2%, $p\leq0.05$) indicating that $PW1^+$ cells are mobilized during PH independently of the experimental model used (Figure 4B).

CH-induced neomuscularization is associated with an increased number of PW1$^+$ cells-derived SMC

We next studied the number of SMC differentiated from PW1$^+$ cells during vascular remodeling in PW1 reporter mice after 4 or 28 days of CH. After 4 days of CH, we observed neomuscularization without any increase in vascular wall thickness whereas after 28 days, both features were observed (Figure 5A and 5B). RVSP was already increased after 4 days of CH while the cardiac right hypertrophy, estimated by the Fulton index, was not modified at 4 days but significantly increased after 28 days of CH (Online Figures VII-A, VII-B, VII-C).

The number of β-gal$^+$ SMC in small pulmonary vessels (<100 µm), as determined by co-immunofluorescence, was significantly increased after 4 days of CH as compared with normoxia indicating an increased percentage of SMC recently derived from PW1$^+$ cells at an early stage during the neomuscularization phase of CH-induced vascular remodeling (Figure 5C). This early increase was confirmed by using a more-specific SMC marker, calponin (CNN1) (Online Figure III). These observations suggest that newly formed SMC during vessel neomuscularization are derived from PW1$^+$ progenitor cells. This is supported by the observation that the number of PW1$^+$ cells (Figure 3B) and of PW1$^+$-derived β-gal$^+$ SMC (Figure 5C) both return to basal levels at 28 days of CH indicating that PW1$^+$ cells and β-gal$^+$ SMC follow similar kinetics. These observations do not exclude the possibility that SMC or myofibroblasts dedifferentiate into PW1-expressing cells during CH to proliferate and further differentiate into SMC. We therefore analyzed mouse lungs for co-expression of PW1 and α-SMA at 0, 1, 2, 3 and 4 days of CH. We found few cells co-expressing both α-SMA and PW1 at all time points (from 2.5 to 7% of all α-SMA$^+$ cells). Overall, few vessels (10-20% of all vessels) contained PW1$^+$/α-SMA$^+$ SMCs. Moreover, we did not observe any increase in the number of PW1$^+$/α-SMA$^+$ cells during the first 4 days of CH (Figure 5D). These results are not in favor of SMC/myofibroblast dedifferentiation into PW1-expressing cells during CH but strongly suggest that newly formed SMC are differentiated from PW1$^+$ progenitor cells recruited during early CH and lose their β-gal expression after 28 days of CH.

Pulmonary PW1$^+$ cells differentiation into vascular SMCs during CH is dependent on the CXCR4 pathway

The SDF-1/CXCR4 pathway is an important regulator of stem and progenitor cells mobilization and homing. We hypothesized that the SDF-1/CXCR4 pathway plays an important role in the recruitment of the pulmonary PW1$^+$ cells during CH. We therefore studied the effect of AMD3100, a CXCR4 antagonist, on PW1$^+$ cells proliferation and differentiation and on vascular remodeling after 4 days of CH. AMD3100 treatment did not modify hematocrit values (data not shown). Based on flow cytometry analysis, we showed that the PW1$^+$ progenitor cells are mainly positive for CXCR4 (Figure 6A). FACS analyses also showed that the number of cells of each PW1$^+$ cell population was not modified by

AMD3100 treatment neither in normoxia nor after CH (Figure 6B). We observed however by co-immunofluorescence that AMD3100 treatment completely prevented the increase in $PW1^+$-derived β-gal^+ vascular SMC obtained after CH but had no effect in normoxia (Figure 6C). These results indicate that the CXCR4 pathway regulates the migration and/or differentiation of $PW1^+$ progenitor cells into vascular SMC but does not regulate $PW1^+$ progenitor cells' proliferation. In addition, AMD3100 treatment partially but significantly inhibited pulmonary vessels neomuscularization during CH without effect during normoxia (Figure 6D). These results indicate that CXCR4 pathway participates in the control of CH-induced neomuscularization.

Resident pulmonary $PW1^+$ cells are recruited during early CH

Previously, we have shown that the BM contains $PW1^+$ cells that correspond to the BM progenitor populations [14]. It has been suggested that the SMC cells that form in the lung in response to CH derive from circulating cells of BM origin [9]. Therefore, we performed a total BM transplantation from PW1-reporter mice crossed with H2B-GFP mice (expressing ubiquitous nuclear GFP fused to histone2B) onto lethally irradiated WT mice. After 8 months, chimerism was evaluated at ~82% (82.2 ± 4.2%, n=10) in the grafted mice blood by FACS analysis of $GFP^+/CD45^+$ blood mononuclear cells (Online Figure VIII). The reconstitution of the $PW1^+/\beta$-gal^+ populations was verified by FACS[14] by comparing the β-gal^+ cells in control PW1-reporter mouse and in mouse transplanted with β-gal^+ BM cells. We observed a similar amount and distribution of β-gal-expressing cells in the BM of control PW1-reporter mouse and in the transplanted mouse indicating that the BM $PW1^+$ cell populations had been efficiently reconstituted in the transplanted mice (Figure 7A). Engrafted mice were then submitted to normoxia or CH for 4 days. CH induced pulmonary vessels neomuscularization as attested by a decreased number of non-muscularized vessels quantified by immunofluorescence (Figure 7B). The percentage of GFP^+/α-SMA^+ cells per vessel in small pulmonary vessels (<100µm) was not modified by CH and we did not detect β-gal^+ cells in the lungs of BM engrafted normoxic or CH mice. These results indicate that circulating GFP^+ BM-derived cells do not contribute to the early pulmonary vascular remodeling. We conclude that newly formed SMC during early CH are not derived from cells originating from the BM (Figure 7C).

$PW1^+$ progenitor cells are present in the human lung and accumulate in remodeled vessels

Our results reveal that a resident population of $PW1^+$ cells is present in the lung that respond to CH and generate SMCs. While the mouse can often serve to unravel cellular events in human disease progression, we set out to determine whether $PW1^+$ cells are present in the human lung and to study them in the pathological context of PAH. We performed immunofluorescence on biopsies obtained from the healthy region of lung samples from cancer patients (control) and on PAH human lung samples. Patients' characteristics are indicated in Online Table I. Similar to our observations from

mouse lungs, we found $PW1^+$ cells in perivascular zones, adjacent to the media of small vessels and in the parenchyma. In contrast to the mouse lungs, $PW1^+$ cells were not scattered but organized in clusters (from 2 to 5 cells) (Figure 8A). In the human PAH lung, we observed $PW1^+$ cells in the perivascular zone of the non-remodeled vessels and only scarce $PW1^+/\alpha\text{-}SMA^+$ cells were found similar to what we observed in the mouse. In the pulmonary remodeled vessels of PAH patients, numerous $PW1^+$ cells were observed in the perivascular area as well as within the vascular wall. We noticed the presence of numerous $PW1^+/\alpha\text{-}SMA^+$ cells in the broad neo-intima or in the thickened media of the remodeled vessels (Figure 8B).

DISCUSSION

Pulmonary arterial hypertension is associated with vascular remodeling and in particular with the neomuscularization of small pulmonary vessels. In this study, we provide *in vitro* and *in vivo* evidence that resident pulmonary PW1$^+$/CD34$^+$ progenitor cells participate in the neomuscularization during CH, an experimental PH model. PW1$^+$ progenitor cells have been isolated in several organs in mouse, human, dog and pigs and share common characteristics with pulmonary PW1$^+$ progenitor cells: 1/ they are able to differentiate into α-SMA$^+$ cells and 2/ they are characterized by the expression of CD34, c-kit and PDGFR-α [14,15,20,22]. These markers have also been used to isolate vascular progenitor cells in other adult organs in rodents and human. In various tissues, resident progenitor cells expressing CD34[10,23,24], c-kit [24,25] or PDGFR-α [25] differentiate into SMC. Resident pulmonary c-kit$^+$ cells in particular have been recently described in human as multipotent stem cells able to generate pulmonary vessels[26]. We also report here the presence of a CD34$^-$/PW1$^+$ population expressing pericyte markers similar to the perivascular progenitor cells identified in multiple human organs [12]. Interestingly, PW1 expression has been recently demonstrated to be essential for progenitor competence in mesoangioblasts that are derived from vessels present in skeletal muscle [20]. Thus, the pulmonary PW1$^+$ cell populations identified here are consistent with previously published vascular progenitor cells and confirm that PW1 identifies multiple progenitor cell populations.

Using PW1-reporter mice [14], we were able to follow the differentiation of these PW1$^+$ progenitor cells into vascular SMC. Although this is not a bona fide lineage-tracing model, the long half-life of β-gal protein ([21] and our own *in vitro* data) allowed us to detect differentiated PW1$^-$ cells derived from PW1$^+$ cells. Our results show that pulmonary resident PW1$^+$ progenitor cells are a novel source of SMC during early CH-induced vascular remodeling. First, we observed an early increase in the number of these progenitor cells and in their proliferation. In addition, we show that one population mobilized during CH will spontaneously differentiate into terminally differentiated SM-MHC$^+$ SMC. Second, we show an increased number of SMC derived from PW1$^+$ cells during early CH-induced neomuscularization. Moreover, CH did not induce expression of PW1 in pulmonary SMC, favoring a model in which direct differentiation of PW1$^+$/α-SMA$^-$ progenitor cells into SMCs occurs as an early response to CH. Last, we demonstrate that these new SMC are not differentiated from BM-derived progenitor cells. Other studies have demonstrated the existence of progenitor cells recruited in a pulmonary pathophysiological context. These studies were performed at late stages of the CH response when vascular remodeling has already concluded. The studies also showed that sustained CH stimulates the mobilization of BM-derived progenitor cells such as mesenchymal stem cells [27], c-kit$^+$ cells [28] and CD11b$^+$ fibrocytes [29] which contribute to pulmonary vessels remodeling [28–30]. Yet, few studies have been able to address the question of the mobilization of resident pulmonary progenitor cells. Long term CH induces the proliferation of resident endothelial progenitor cells in the mouse lung [31]. Lineage-tracing experiments have shown that a perivascular lung mesenchymal stem cell population contributes to microvascular

remodeling after 5 weeks of hypobaric hypoxia [32]. Ricard *et al.*[7] showed that $NG2^+$ pericytes which contribute to forming SMC-like cells, are increased from day 7 to day 21 of CH demonstrating a later and more progressive recruitment of these cells in this model. This is consistent with our results, which indicate that the number of $PW1^+/CD34^-/CD146^+$ cells (84% $NG2^+$) is not significantly increased after 4 days of CH. Very recently, Sheikh *et al.* [5] have demonstrated that muscularization of specific distal arteries arise from the migration and clonal proliferation of vascular PDGFR-β^+/α-SMA^+ cells observed between 3 and 7 days of CH. However, after 3 days of CH, distal arterioles were barely muscularized and contained very few proliferating SMCs. These results cannot explain the high level of neomuscularization already observed after 2 or 4 days of CH ([33] and our results). Yet, we showed that after 4 days of CH, resident proliferating $PW1^+$ progenitor cells are important contributors of new SMC. Indeed, $PW1^+$ cells represent 50% of all the proliferating cells found in the lung parenchyma after 4 days of CH (data not shown). Therefore, altogether our results with previous ones[5,7], suggest that hypoxia-induced pulmonary vessels muscularization is dependent on multiple resident SMC sources recruited successively: $PW1^+/CD34^+$ progenitor cells, PDGFR-β^+ SMC and $NG2^+$ pericytes. Other investigations have also reported significant recruitment of resident perivascular progenitor cells during vascular remodeling/pathophysiology such as the restenosis [34] or the atherosclerosis [35]. These resident progenitor cells contribute to maintain the tissue homeostasis and integrity and were proposed to be responsible for pathological features such as the SMCs-like accumulation in remodeled vessels [9].

The SDF-1/CXCR4 pathway is one of the major regulators of progenitor and stem cells recruitment and homing [36]. In addition, pulmonary concentrations of CXCR4 ligands stromal-derived factor 1 (SDF-1) and macrophage migration inhibitory factor (MIF) were found to be elevated during CH [37,38] and CXCR4 inhibition by AMD3100 treatment was shown to partially prevent CH-induced increase in media thickness[30]. Consistent with these results, we here show that the increase in the number of $PW1^+$-derived SMC and the neomuscularization are blocked by AMD3100, indicating that they are dependent on the CXCR4 pathway. Although we cannot prove yet whether $PW1^+$ progenitor cells are directly activated through the CXCR4 receptor, our observation that most $PW1^+$ progenitor cells express CXCR4 suggests that the CXCR4 ligand may directly attract them to the vessels. Interestingly, our result shows that the CXCR4 pathway regulates $PW1^+$ progenitor cells migration and/or differentiation but not their proliferation. This result is consistent with the major homing effect of the SDF-1/CXCR4 pathway but this indicates that further studies are needed to understand which factors are responsible for inducing proliferation of $PW1^+$ progenitor cells during early CH. It would be particularly interesting to study the effect of PAH-specific drugs on the proliferation, migration and differentiation of $PW1^+$ cells or to target pathways which regulate pulmonary vascular remodeling such as serotonin, PDGF or HIF-1α pathways [39].

We report here a similar increase in the number of lung parenchymal $PW1^+$ cells in two well-recognized and widely used experimental models, the MCT- and the CH-induced PH models. Both models induce

inflammation as an initial process [40,41] and inflammatory cytokines, such as MCP-1, TNF-α or IL-10, play a crucial role in the proliferation and differentiation capacities of stem/progenitor cells [42]. Another common mechanism between the two models could involve HIF-1α as it is well established that inflammation causes a hypoxia-independent HIF-1α activation in response to the pro-inflammatory IL-1β [43]. HIF-1α regulates stem cells mobilization [44] and could therefore be involved in the recruitment of $PW1^+$ progenitor cells.

Finally, we demonstrate the presence of the $PW1^+$ cells in the parenchyma and perivascular zones in the control human lung. Remarkably, these cells are found as small perivascular clusters similar to pulmonary c-kit^+ cells as observed by Kajstura *et al.* [26]. These $PW1^+$ progenitor cells were mainly absent from non-remodeled vessel walls but we found numerous $PW1^+$ cells within the vascular wall and perivascular zone of the remodeled vessels in PAH patients. This result confirms previous observations that progenitor cells are present in remodeled pulmonary arteries in lung tissues from PAH patients [45,46]. Interestingly, numerous $PW1^+$/α-SMA^+ cells were present in the hypertrophic media and in the neointima. We did not observe these features in the mouse lung vessels after 28 days of CH (data not shown). As human PAH lung samples are obtained from transplanted patients with an end-stage disease, the severe inflammatory context and the proliferative and SMC-like/myofibroblast dedifferentiation conditions could be involved in maintaining the PW1 expression in these mature and dysfunctional cells. This is supported by the sustained increase in the number of pulmonary $PW1^+$ cells observed in the MCT treated-rat model after 21 days whereas in the chronic hypoxic mouse model this number is back to control levels after 28 days of CH. This suggests that the sustained mobilization of pulmonary $PW1^+$ cells is associated with the severity of the PH disease.

In conclusion, we show here that the lung contains three myogenic $PW1^+$ progenitor cell populations that are resident in parenchymal and perivascular zones in the adult mouse lung. Based on their myogenic capacities both *in vivo* and *in vitro*, and on our immunofluorescence and FACS observations on normoxic and CH-submitted mouse lungs, we suggest that the three pulmonary $PW1^+$ cell populations are a source of vascular smooth muscle progenitor cells in the adult mouse lung and that the $PW1^+$/$CD34^+$/c-kit^+ and the $PW1^+$/$CD34^+$/c-kit^-/PDGFR-α^+ cell populations are important players in neomuscularization during CH via activation of the CXCR4 pathway. However, our results do not allow to determine the respective roles of each $PW1^+$ cell population. Strategies aiming to inhibit the mobilization, proliferation or differentiation of these cells, may provide important therapeutic avenues leading to an early treatment of PAH.

Acknowledgements

We are grateful to Luigi Formicola, Piera Smeriglio, David Ollitrault, Nadine Suffee-Mosbah, Dorota Jeziorowska, Svetlana Maugenre, Heïdi Brisson and Inès Bouchareb for helpful suggestions and/or technical support, and Catherine Blanc and Aurélien Corneau for assistance with FACS.

Funding

This work was supported by Institute of Cardiometabolism and Nutrition (ICAN) (ANR-10-IAHU-05). D.S., G.M. and J.S.H. are supported by a grant from the Fondation Leducq (grant 13CVD01, CardioStemNet project). S.N. acknowledges support from the Agence Nationale de la Recherche (ANR-15-CE14-0020-01). F.D. is supported was supported by the French Ministry of Research and Education. This project also received support from OPTISTEM (Optimization of stem cell therapy for degenerative epithelial and muscle diseases contract number Health-F5-2009-223098) and ENDOSTEM (Activation of vasculature associated stem cells and muscle stem cells for the repair and maintenance of muscle tissue-agreement number 241440). D.S. acknowledges support from the Institut Pasteur and the Agence Nationale de la Recherche (Laboratoire d'Excellence Revive, Investissement d'Avenir; ANR-10-LABX-73). MH acknowledges support from the Assistance Publique Hôpitaux de Paris (Département Hospitalo-Universitaire Thorax Innovation, DHU TORINO) and the Agence Nationale de la Recherche (Labex LERMIT).

Disclosures

None.

References

1. Galiè N, Humbert M, Vachiery J-L *et al.* 2015 ESC/ERS Guidelines for the diagnosis and treatment of pulmonary hypertension. *Eur Respir J*. 2015;46:903-975.
2. Stenmark KR, Mecham RP. Cellular and molecular mechanisms of pulmonary vascular remodeling. *Annu Rev Physiol*. 1997;59:89-144.
3. Rabinovitch M. Molecular pathogenesis of pulmonary arterial hypertension. *J Clin Invest*. 2012;122:4306-4313.
4. Guignabert C, Dorfmuller P. Pathology and pathobiology of pulmonary hypertension. *Semin Respir Crit Care Med*. 2013;34:551-559
5. Sheikh AQ, Misra A, Rosas IO, Adams RH, Greif DM. Smooth muscle cell progenitors are primed to muscularize in pulmonary hypertension. *Sci Transl Med*. 2015;7:308ra159.
6. Meyrick B, Reid L. Ultrastructural findings in lung biopsy material from children with congenital heart defects. *Am J Pathol*. 1980;101:527-542.
7. Ricard N, Tu L, Le Hiress M, Huertas A, Phan C, Thuillet R, Sattler C, Fadel E, Seferian A, Montani D, Dorfmüller P, Humbert M, Guignabert C. Increased pericyte coverage mediated by endothelial-derived fibroblast growth factor-2 and interleukin-6 is a source of smooth muscle-like cells in pulmonary hypertension. *Circulation*. 2014;129:1586-1597.
8. Ranchoux B, Antigny F, Rucker-Martin C *et al.* Endothelial-to-mesenchymal transition in pulmonary hypertension. *Circulation*. 2015;131:1006-1018.
9. Yeager ME, Frid MG, Stenmark KR. Progenitor cells in pulmonary vascular remodeling. *Pulm Circ*. 2011;1:3-16.
10. Psaltis PJ, Simari RD. Vascular wall progenitor cells in health and disease. *Circ Res*. 2015;116(8):1392-1412.
11. Chong JJH, Reinecke H, Iwata M, Torok-Storb B, Stempien-Otero A, Murry CE. Progenitor cells identified by PDGFR-alpha expression in the developing and diseased human heart. *Stem Cells Dev*. 2013;22:1932-1943.
12. Crisan M, Yap S, Casteilla L *et al.* A perivascular origin for mesenchymal stem cells in multiple human organs. *Cell Stem Cell*. 2008;3:301-313.
13. Mitchell KJ, Pannerec A, Cadot B, Parlakian A, Besson V, Gomes ER, Marazzi G, Sassoon DA. Identification and characterization of a non-satellite cell muscle resident progenitor during postnatal development. *Nat Cell Biol*. 2010;12:257-266.
14. Besson V, Smeriglio P, Wegener A, Relaix F, Nait Oumesmar B, Sassoon DA, Marazzi G. PW1 gene/paternally expressed gene 3 (PW1/Peg3) identifies multiple adult stem and progenitor cell populations. *Proc Natl Acad Sci U A*. 2011;108:11470-11475.
15. Pannérec A, Formicola L, Besson V, Marazzi G, Sassoon DA. Defining skeletal muscle resident progenitors and their cell fate potentials. *Dev Camb Engl*. 2013;140:2879-2891.
16. Relaix F, Wei XJ, Wu X, Sassoon DA. Peg3/Pw1 is an imprinted gene involved in the TNF-NFkappaB signal transduction pathway. *Nat Genet*. 1998;18:287-291.
17. Relaix F, Wei X, Li W, Pan J, Lin Y, Bowtell DD, Sassoon DA, Wu X. Pw1/Peg3 is a potential cell death mediator and cooperates with Siah1a in p53-mediated apoptosis. *Proc Natl Acad Sci U A*. 2000;97:2105-2110.
18. Jiang X, Yu Y, Yang HW, Agar NYR, Frado L, Johnson MD. The imprinted gene PEG3 inhibits Wnt signaling and regulates glioma growth. *J Biol Chem*. 2010;285:8472-8480.
19. Thiaville MM, Huang JM, Kim H, Ekram MB, Roh T-Y, Kim J. DNA-binding motif and target genes of the imprinted transcription factor PEG3. *Gene*. 2013;512:314-320.
20. Bonfanti C, Rossi G, Tedesco FS, Giannotta M, Benedetti S, Tonlorenzi R, Antonini S, Marazzi G, Dejana E, Sassoon D, Cossu G, Messina G. PW1/Peg3 expression regulates key properties that determine mesoangioblast stem cell competence. *Nat Commun*. 2015;6:6364.
21. Bachmair A, Finley D, Varshavsky A. In vivo half-life of a protein is a function of its

amino-terminal residue. *Science*. 1986;234:179-186.
22. Lewis FC, Henning BJ, Marazzi G, Sassoon D, Ellison GM, Nadal-Ginard B. Porcine skeletal muscle-derived multipotent PW1pos/Pax7neg interstitial cells: isolation, characterization, and long-term culture. *Stem Cells Transl Med*. 2014;3:702-712.
23. Wu Y, Shen Y, Kang K, Zhang Y, Ao F, Wan Y, Song J. Effects of estrogen on growth and smooth muscle differentiation of vascular wall-resident CD34(+) stem/progenitor cells. *Atherosclerosis*. 2015;240:453-461.
24. Ellison GM, Vicinanza C, Smith AJ *et al.* Adult c-kit(pos) cardiac stem cells are necessary and sufficient for functional cardiac regeneration and repair. *Cell*. 2013;154:827-842.
25. Chong JJH, Reinecke H, Iwata M, Torok-Storb B, Stempien-Otero A, Murry CE. Progenitor cells identified by PDGFR-alpha expression in the developing and diseased human heart. *Stem Cells Dev*. 2013;22:1932-1943.
26. Kajstura J, Rota M, Hall SR *et al.* Evidence for human lung stem cells. *N Engl J Med*. 2011;364:1795-1806.
27. Rochefort GY, Delorme B, Lopez A, Hérault O, Bonnet P, Charbord P, Eder V, Domenech J. Multipotential mesenchymal stem cells are mobilized into peripheral blood by hypoxia. *Stem Cells Dayt Ohio*. 2006;24:2202-2208.
28. Davie NJ, Crossno JT, Frid MG, Hofmeister SE, Reeves JT, Hyde DM, Carpenter TC, Brunetti JA, McNiece IK, Stenmark KR. Hypoxia-induced pulmonary artery adventitial remodeling and neovascularization: contribution of progenitor cells. *Am J Physiol - Lung Cell Mol Physiol*. 2004;286:L668-L678.
29. Frid MG, Brunetti JA, Burke DL, Carpenter TC, Davie NJ, Reeves JT, Roedersheimer MT, van Rooijen N, Stenmark KR. Hypoxia-induced pulmonary vascular remodeling requires recruitment of circulating mesenchymal precursors of a monocyte/macrophage lineage. *Am J Pathol*. 2006;168:659-669.
30. Gambaryan N, Perros F, Montani D, Cohen-Kaminsky S, Mazmanian M, Renaud JF, Simonneau G, Lombet A, Humbert M. Targeting of c-kit+ haematopoietic progenitor cells prevents hypoxic pulmonary hypertension. *Eur Respir J*. 2011;37:1392-1399.
31. Nishimura R, Nishiwaki T, Kawasaki T, Sekine A, Suda R, Urushibara T, Suzuki T, Takayanagi S, Terada J, Sakao S, Tatsumi K. Hypoxia-induced proliferation of tissue-resident endothelial progenitor cells in the lung. *Am J Physiol Lung Cell Mol Physiol*. 2015;308:L746-L758.
32. Chow K, Fessel JP, Kaoriihida-Stansbury, Schmidt EP, Gaskill C, Alvarez D, Graham B, Harrison DG, Wagner DH Jr, Nozik-Grayck E, West JD, Klemm DJ, Majka SM. Dysfunctional resident lung mesenchymal stem cells contribute to pulmonary microvascular remodeling. *Pulm Circ*. 2013;3:31-49.
33. Quinlan TR, Li D, Laubach VE, Shesely EG, Zhou N, Johns RA. eNOS-deficient mice show reduced pulmonary vascular proliferation and remodeling to chronic hypoxia. *Am J Physiol Lung Cell Mol Physiol*. 2000;279:L641-L650.
34. Tigges U, Komatsu M, Stallcup WB. Adventitial pericyte progenitor/mesenchymal stem cells participate in the restenotic response to arterial injury. *J Vasc Res*. 2013;50:134-144.
35. Hu Y, Zhang Z, Torsney E, Afzal AR, Davison F, Metzler B, Xu Q. Abundant progenitor cells in the adventitia contribute to atherosclerosis of vein grafts in ApoE-deficient mice. *J Clin Invest*. 2004;113:1258-1265.
36. Nagasawa T. CXC chemokine ligand 12 (CXCL12) and its receptor CXCR4. *J Mol Med Berl Ger*. 2014;92:433-439.
37. Young KC, Torres E, Hatzistergos KE, Hehre D, Suguihara C, Hare JM. Inhibition of the SDF-1/CXCR4 Axis Attenuates Neonatal Hypoxia-Induced Pulmonary Hypertension. *Circ Res*. 2009;104:1293-1301.

38. Zhang Y, Talwar A, Tsang D, Bruchfeld A, Sadoughi A, Hu M, Omonuwa K, Cheng KF, Al-Abed Y, Miller EJ. Macrophage migration inhibitory factor mediates hypoxia-induced pulmonary hypertension. *Mol Med Camb Mass*. 2012;18:215-223.
39. Montani D, Chaumais M-C, Guignabert C, Günther S, Girerd B, Jaïs X, Algalarrondo V, Price LC, Savale L, Sitbon O, Simonneau G, Humbert M. Targeted therapies in pulmonary arterial hypertension. *Pharmacol Ther*. 2014;141:172-191.
40. Vergadi E, Chang MS, Lee C, Liang OD, Liu X, Fernandez-Gonzalez A, Mitsialis SA, Kourembanas S. Early macrophage recruitment and alternative activation are critical for the later development of hypoxia-induced pulmonary hypertension. *Circulation*. 2011;123:1986-1995.
41. Wilson DW, Segall HJ, Pan LC, Dunston SK. Progressive inflammatory and structural changes in the pulmonary vasculature of monocrotaline-treated rats. *Microvasc Res*. 1989;38:57-80.
42. Kizil C, Kyritsis N, Brand M. Effects of inflammation on stem cells: together they strive? *EMBO Rep*. 2015;16:416-426.
43. Stasinopoulos I, O'Brien DR, Bhujwalla ZM. Inflammation, but not hypoxia, mediated HIF-1alpha activation depends on COX-2. *Cancer Biol Ther*. 2009;8:31-35.
44. Liu L, Yu Q, Lin J, Lai X, Cao W, Du K, Wang Y, Wu K, Hu Y, Zhang L, Xiao H, Duan Y, Huang H. Hypoxia-inducible factor-1α is essential for hypoxia-induced mesenchymal stem cell mobilization into the peripheral blood. *Stem Cells Dev*. 2011;20:1961-1971.
45. Majka SM, Skokan M, Wheeler L, Harral J, Gladson S, Burnham E, Loyd JE, Stenmark KR, Varella-Garcia M, West J. Evidence for cell fusion is absent in vascular lesions associated with pulmonary arterial hypertension. *Am J Physiol Lung Cell Mol Physiol*. 2008;295:L1028-L1039.
46. Montani D, Perros F, Gambaryan N, Girerd B, Dorfmuller P, Price LC, Huertas A, Hammad H, Lambrecht B, Simonneau G, Launay JM, Cohen-Kaminsky S, Humbert M. C-kit-positive cells accumulate in remodeled vessels of idiopathic pulmonary arterial hypertension. *Am J Respir Crit Care Med*. 2011;184:116-123.

Figure legends

Figure 1: Mouse lung $PW1^+$ cells are present in perivascular and parenchymal zones and express progenitor and pericyte markers. **(A)** Immunofluorescent staining on mouse lung for PW1 (green) and vWF (endothelial marker) (red) and **(B)** for PW1 (red) and α-SMA (SMC marker) (green) reveals $PW1^+$ cells in parenchyma and perivascular zones (white arrowheads). **(C)** Three $PW1^+$ cell populations were sorted by FACS based on cell surface markers expression profiles and β-galactosidase activity: $PW1^+/CD34^+/c\text{-}kit^+$ cells, $PW1^+/CD34^+/c\text{-}kit^-/PDGFR\text{-}\alpha^+$ cells and $PW1^+/CD34^-/CD146^+$ cells. PDGFR-α and CD146 expression were also measured by FACS on these cell populations. **(D)** PW1 expression (green) was confirmed in sorted cells and the mean percentage of $PW1^+$ cells is indicated. Representative images from mouse lung sorted cytospun cells (n=4). **(E)** Co-localization of PW1 (green) and c-kit, PDGFR-α and CD146 (red) were confirmed on mouse lung by immunofluorescence. Yellow arrowheads indicate cells co-expressing PW1 and other progenitor markers. L: Lumen of vessel. Confocal microscopy. Scale bars: 20μm.

Figure 2: The mouse lung $PW1^+$ cells differentiate into smooth muscle cells (SMC). **(A)** FACS isolated $PW1^+$ populations immunostained directly after sorting for SMC markers α-SMA (green) and SM-MHC (red) show no staining. **(B)** FACS isolated $PW1^+$ cell populations immunostained after culture show staining for SMC markers α-SMA (green) and SM-MHC (red). $PW1^+/CD34^+/c\text{-}kit^+$ and $PW1^+/CD34^-/CD146^+$ cells differentiation was induced by addition of TGF-β_1 and PDGF-BB whereas $PW1^+/CD34^+/c\text{-}kit^-/PDGFR\text{-}\alpha^+$ cells were left without induction. Representative images of multiple experiments (n=3). Confocal microscopy. **(C)** Mouse lungs immunostained for β-gal (red) and for SMC markers α-SMA, calponin CNN1 or SM-MHC (green) show that multiple SMC express β-gal in the media of pulmonary vessels (yellow arrowheads). L: Lumen of vessel. Epifluorescence acquisition followed by deconvolution and z axis-projection of stacked images. Scale bars: 20μm.

Figure 3: $PW1^+$ progenitor cells are recruited and proliferate during early CH in mouse. **(A)** Quantitative analysis of lung $PW1^+$ cell populations from mice in normoxia (N, n=22) versus 4 days of CH (CH 4d, n=15). The mean percentage of total viable cells for each $PW1^+$ cell population was measured by FACS in normoxic and CH lungs. Values are means ± SEM, **** $p<0.0001$ vs N (two-tailed MW). **(B)** Quantification of $PW1^+$ cells in lung parenchyma from normoxic or CH mice. a) Representative images of lung parenchyma from normoxic and CH mice stained for PW1 (PW1 in red, positive cells are marked by white arrowheads). b) The percentage of lung $PW1^+$ cells per field from mice submitted to normoxia and CH for 4 or 28 days was measured by immunofluorescence (n=3 for each condition). Values are means ± SEM, * $p<0.05$ vs N (KW-Dunn). **(C)** Quantification of proliferating $PW1^+$ cells in lung parenchyma from N or CH 4d mice. a) Representative images of lung parenchyma from normoxic and hypoxic mice stained for PW1 (green) and BrdU (red) (double positive are marked by yellow arrowheads). b) The percentage of lung $BrdU^+$ proliferating $PW1^+$ cells was determined by immunofluorescence (n=5 for each condition). Values are means ± SEM, ** $p<0.01$ vs N (two-tailed MW). Confocal microscopy. Scale bars: 20μm. ns: non significant.

Figure 4: Lung $PW1^+$ progenitor cells are also recruited in another PAH model: the monocrotaline-injected rat. **(A)** Representative images of control and monocrotaline-injected rat lungs stained with anti-PW1 antibody (green, white arrowheads). **(B)** Quantification by immunofluorescence of the percentage of $PW1^+$ cells from control (saline) and monocrotaline injected-rat lungs (MCT 21d) (n=3). Epifluorescence microscopy. Scale bars: 20μm. Values are means ± SEM,* $p\leq0.05$ versus Saline (one-tailed MW).

Figure 5: CH-induced neomuscularization is associated with an increased number of $PW1^+$-derived SMC. **(A)** Pulmonary vessel muscularization and **(B)** medial thickening of muscularized pulmonary vessels were determined by immunofluorescence in lungs from normoxic (N) or chronic hypoxic (CH 4d) mice using anti-α-SMA and anti-vWF antibodies (n=5 to 7). For each animal, more than 100 vWF^+

vessels (<100 μm) were analyzed for muscularization (α-SMA$^+$). NM for non-, PM for partially- and FM for fully-muscularized. **(C)** Quantification of lung β-gal-expressing SMC in normoxic and CH mice. a) Representative images of lungs from normoxic (N) or chronic hypoxic (CH 4d and CH 28d) mice stained with β-gal (red) and α-SMA (green). b) The percentage of lung β-gal$^+$/α-SMA$^+$ cells (yellow arrowheads) in fully muscularized vessels (<100 μm) was determined by immunofluorescence in normoxic (n=5), CH 4 days (n=4) and CH 28 days (n=4) mice. **(D)** Quantification of vascular PW1$^+$/α-SMA$^+$ cells in pulmonary vessels of normoxic mice (N) and of mice submitted to 1 to 4 days of CH (CH1d to CH4d), using anti-PW1, and anti-α-SMA antibodies (n=3 for each condition). L: Lumen of vessel. Confocal microscopy. Scale bars: 20μm. Values are means ± SEM,*p<0.05, **p<0.01 versus N, ns: non significant (KW-Dunn).

Figure 6: AMD3100 inhibits differentiation of PW1$^+$ progenitor cells into vascular SMCs but not their proliferation. **(A)** CXCR4 expression was measured by FACS on the PW1$^+$/CD34$^-$/CD146$^+$ and the PW1$^+$/CD34$^+$ cell populations. The percentage of CXCR4$^+$ cells for each population is indicated. SSC: side scatter area. **(B)** Quantitative analysis of lung PW1$^+$/CD34$^+$ cell populations from normoxic (N) or chronic hypoxic (CH 4d) mice treated with AMD3100 or saline. The mean percentage of total viable cells for each PW1$^+$ cell population was measured by FACS. **(C)** The percentage of lung β-gal$^+$/α-SMA$^+$ in fully muscularized vessels (<100 μm) from mice treated with AMD3100 or saline and submitted to normoxia (n=4) or CH for 4 days (n=7), was measured by immunofluorescence. **(D)** Pulmonary vessel muscularization (percentage of fully and partially muscularized vessels) was determined by immunofluorescence in lungs from normoxic (N) or chronic hypoxic (CH 4d) mice treated with AMD3100 or saline, using anti-α-SMA and anti-vWF (n=4 to 7/group). For each animal, more than 50 vWF$^+$ vessels (<100 μm) were analyzed for muscularization (α-SMA$^+$). Values are means ± SEM, * p<0.05, ** p<0,01, *** p<0.001 CH vs N and $ p<0.05 AMD3100 vs saline, ns: non significant (KW-Dunn).

Figure 7: The pulmonary PW1$^+$ cells recruited early in the CH mouse are not derived from bone marrow. **(A)** Flow cytometry analysis of the engrafted BM cells 6 months after transplantation compared with BM cells from a control PW1-reporter mouse (CTRL). Sca-1$^+$/c-kit$^-$ (Q1), Sca-1$^+$/c-kit$^+$ (Q2) and Sca-1$^-$/c-kit$^+$ (Q4) cells were analyzed for β-gal activity[14]. The percentage for each population is indicated in percentage of parent. **(B)** Pulmonary vessels muscularization was determined by immunofluorescence using anti-α-SMA and anti-vWF on lungs of normoxic (N) and chronic hypoxic (CH 4d) transplanted mice (n=5). NM for non-, PM for partially- and FM for fully-muscularized. For each animal, more than 50 vWF$^+$ vessels (<100 μm) were analyzed for muscularization (α-SMA$^+$). Vessels showing a perimeter with more than 90% of muscularization were considered fully muscularized. Values are means ± SEM, *p<0.05, **p<0.01 (two-tailed MW N vs CH 4d). **(C)** Quantification of BM-derived SMC in pulmonary vessels of normoxic (N) and hypoxic (CH 4d or CH

21d) mice, using anti-GFP, anti-β-gal and anti-α-SMA antibodies. The percentage of α-SMA$^+$/GFP$^+$ SMCs derived from BM were similar in the transplanted mice lungs under normoxia (N) and after 4 days of chronic hypoxia (CH 4d) (n=5). Confocal microscopy. Scale bars: 20μm. Values are means ± SEM, (two-tailed MW). ns: non significant.

Figure 8: The PW1$^+$ progenitor cells are also present in the human lung and are numerous around and within the remodelled vessels of PAH patients. Human lung sections were stained for α-SMA (red) and PW1 (green). Images are representative of lung tissues from control lungs (n=3) **(A)** and from patients with pulmonary arterial hypertension (n=3) **(B)**. We noticed the presence of PW1$^+$ cells in parenchyma from control lung tissues and in perivascular zones from both control and PAH lung tissues **(A, B1 and B3)** (white stars). In pulmonary arterial lesions of patients with PAH, we showed the presence of PW1$^+$ cells expressing α-SMA$^+$ in the neo-intima (yellow stars) **(B2)**, and in the non-thickened **(B2)** and hypertrophic **(B4)** media (yellow arrowheads). L: lumen of vessel, n: neo-intima and m: media, White dotted line: autofluorescent internal elastic lamina. Confocal microscopy. Scale bars: 20μm.

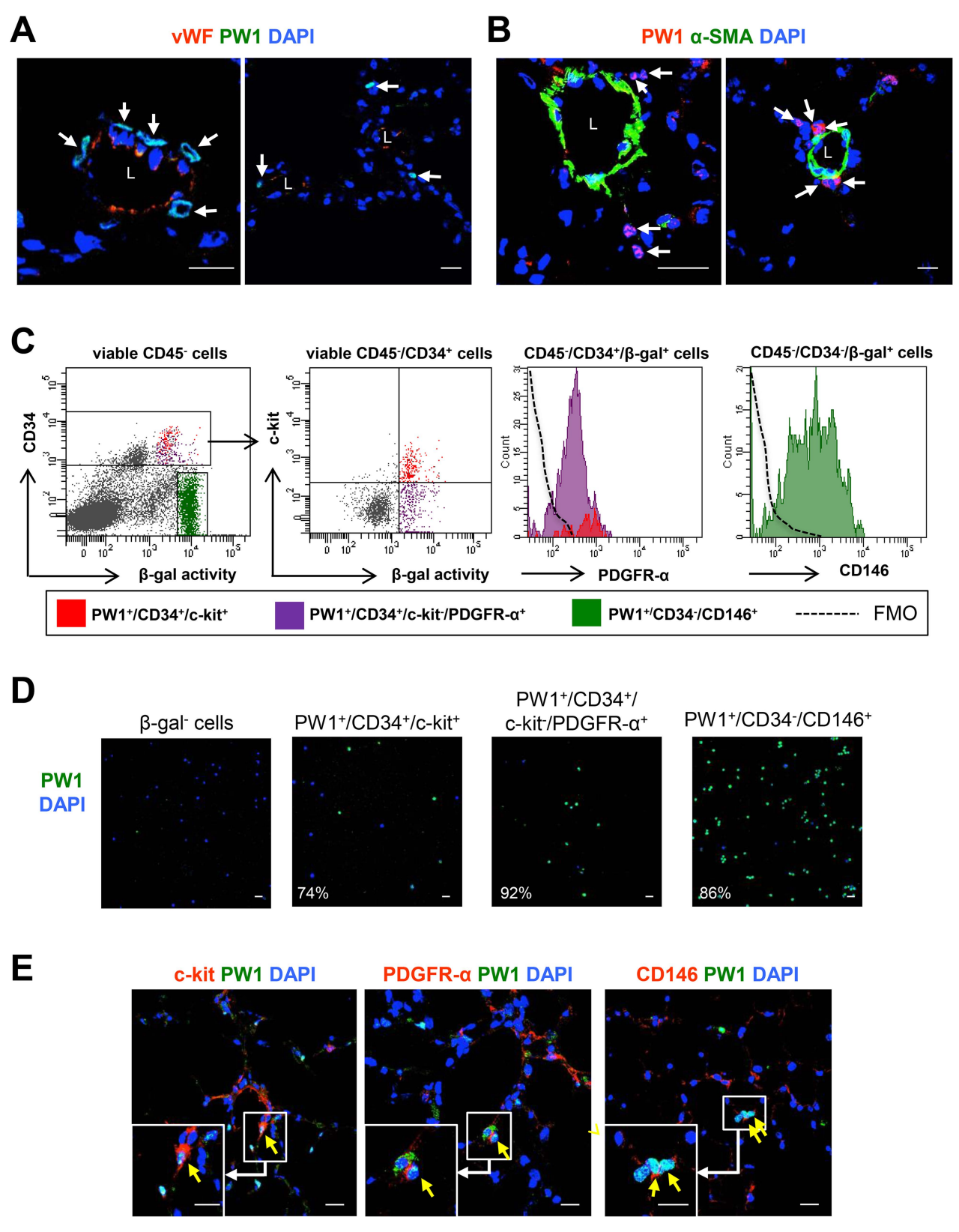
A
vWF PW1 DAPI
L
L
B
PW1 α-SMA DAPI
L
L
C
viable CD45- cells
CD34
β-gal activity
viable CD45-/CD34+ cells
c-kit
β-gal activity
CD45-/CD34+/β-gal+ cells
Count
PDGFR-α
CD45-/CD34-/β-gal+ cells
Count
CD146
PW1+/CD34+/c-kit+
PW1+/CD34+/c-kit-/PDGFR-α+
PW1+/CD34-/CD146+
FMO
D
β-gal- cells
PW1+/CD34+/c-kit+
PW1+/CD34+/
c-kit-/PDGFR-α+
PW1+/CD34-/CD146+
PW1
DAPI
74%
92%
86%
E
c-kit PW1 DAPI
PDGFR-α PW1 DAPI
CD146 PW1 DAPI

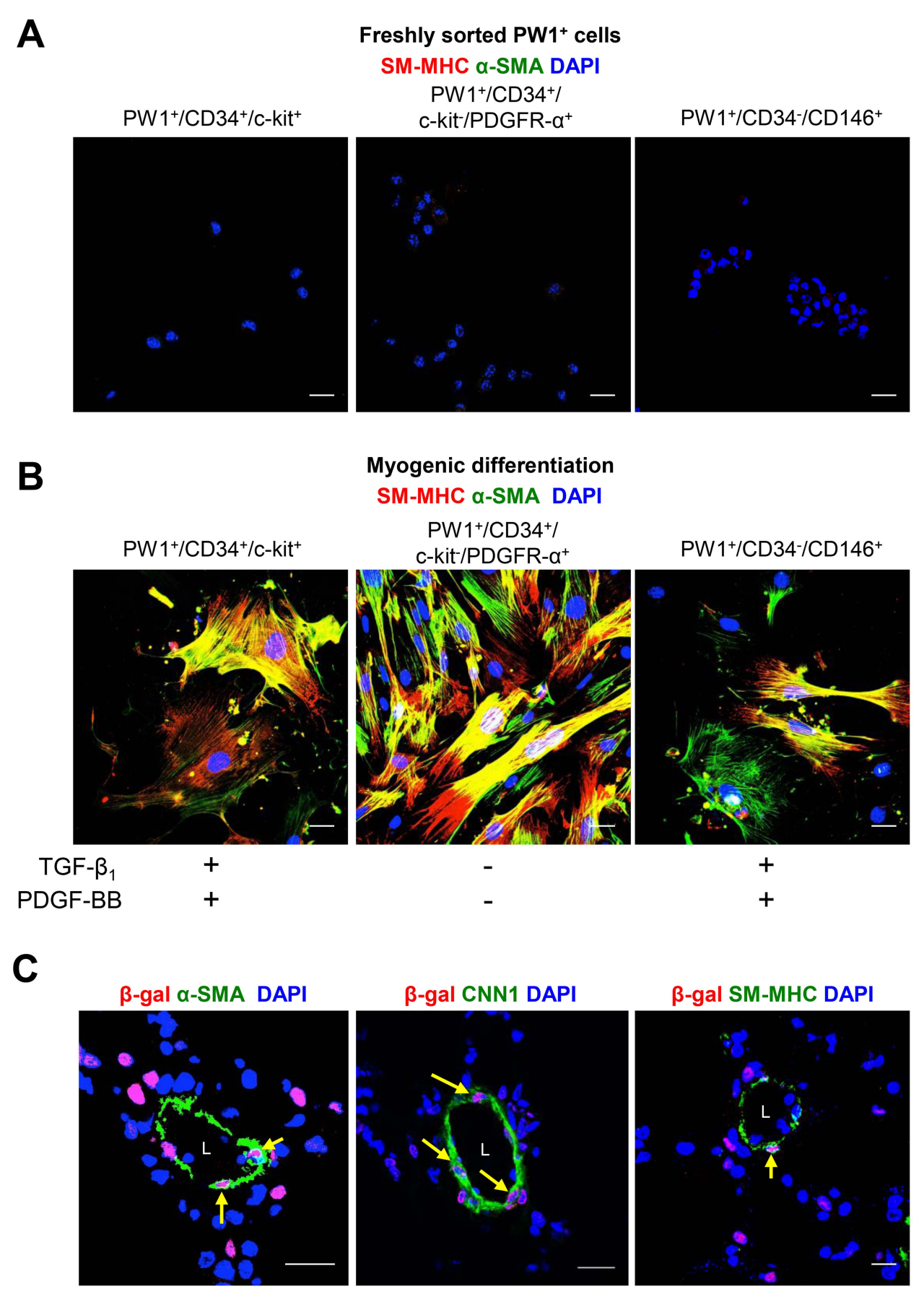
A
Freshly sorted PW1+ cells
SM-MHC α-SMA DAPI
PW1+/CD34+/c-kit+
PW1+/CD34+/
c-kit-/PDGFR-α+
PW1+/CD34-/CD146+
B
Myogenic differentiation
SM-MHC α-SMA DAPI
PW1+/CD34+/c-kit+
PW1+/CD34+/
c-kit-/PDGFR-α+
PW1+/CD34-/CD146+
TGF-β1 + - +
PDGF-BB + - +
C
β-gal α-SMA DAPI
β-gal CNN1 DAPI
β-gal SM-MHC DAPI
L
L
L

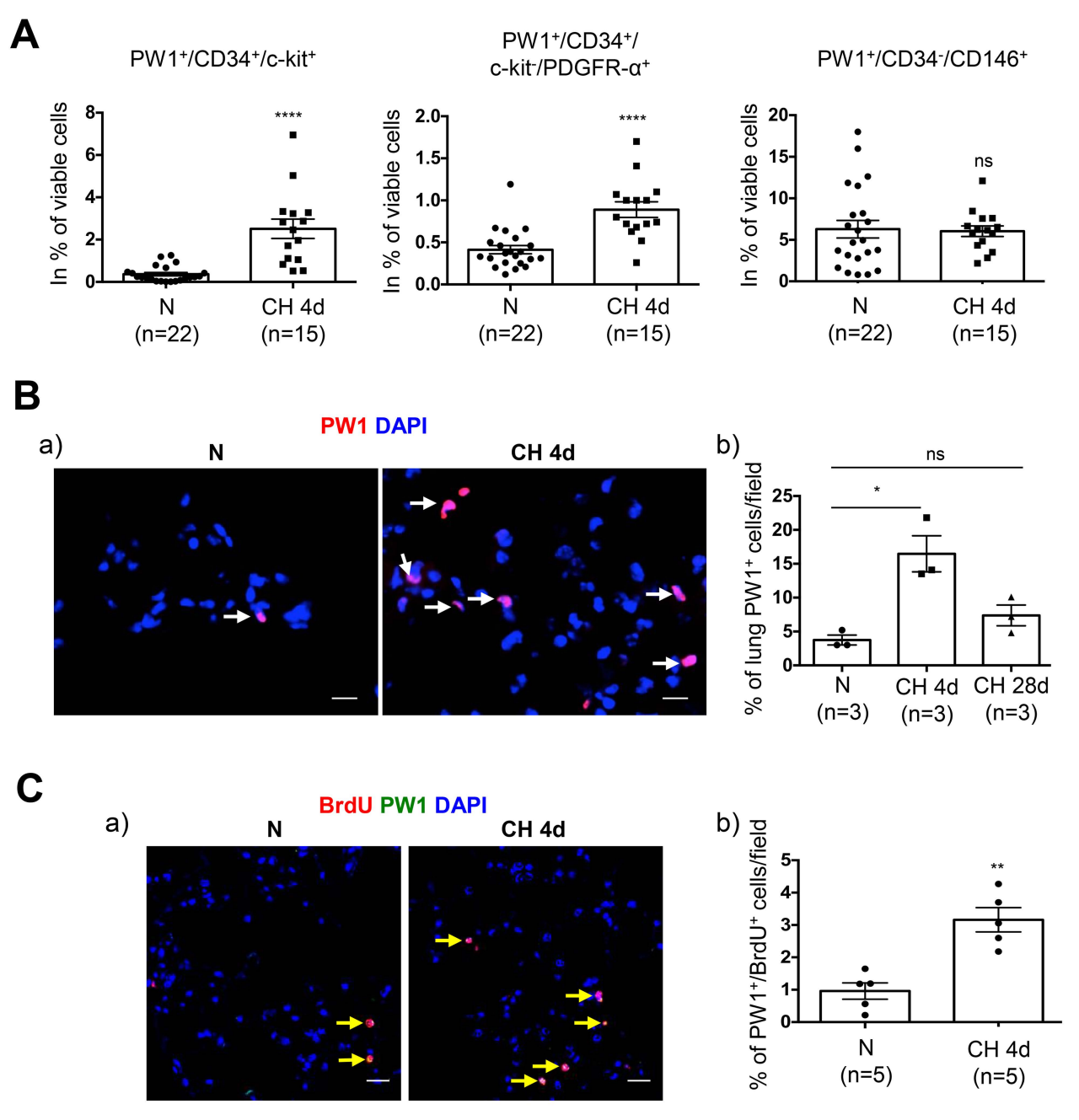
A
PW1+/CD34+/c-kit+
PW1+/CD34+/
c-kit-/PDGFR-α+
PW1+/CD34-/CD146+
ln % of viable cells
****
****
ns
N
(n=22)
CH 4d
(n=15)
B
PW1 DAPI
a)
N
CH 4d
b)
ns
*
% of lung PW1+ cells/field
N
(n=3)
CH 4d
(n=3)
CH 28d
(n=3)
C
BrdU PW1 DAPI
a)
N
CH 4d
b)
**
% of PW1+/BrdU+ cells/field
N
(n=5)
CH 4d
(n=5)

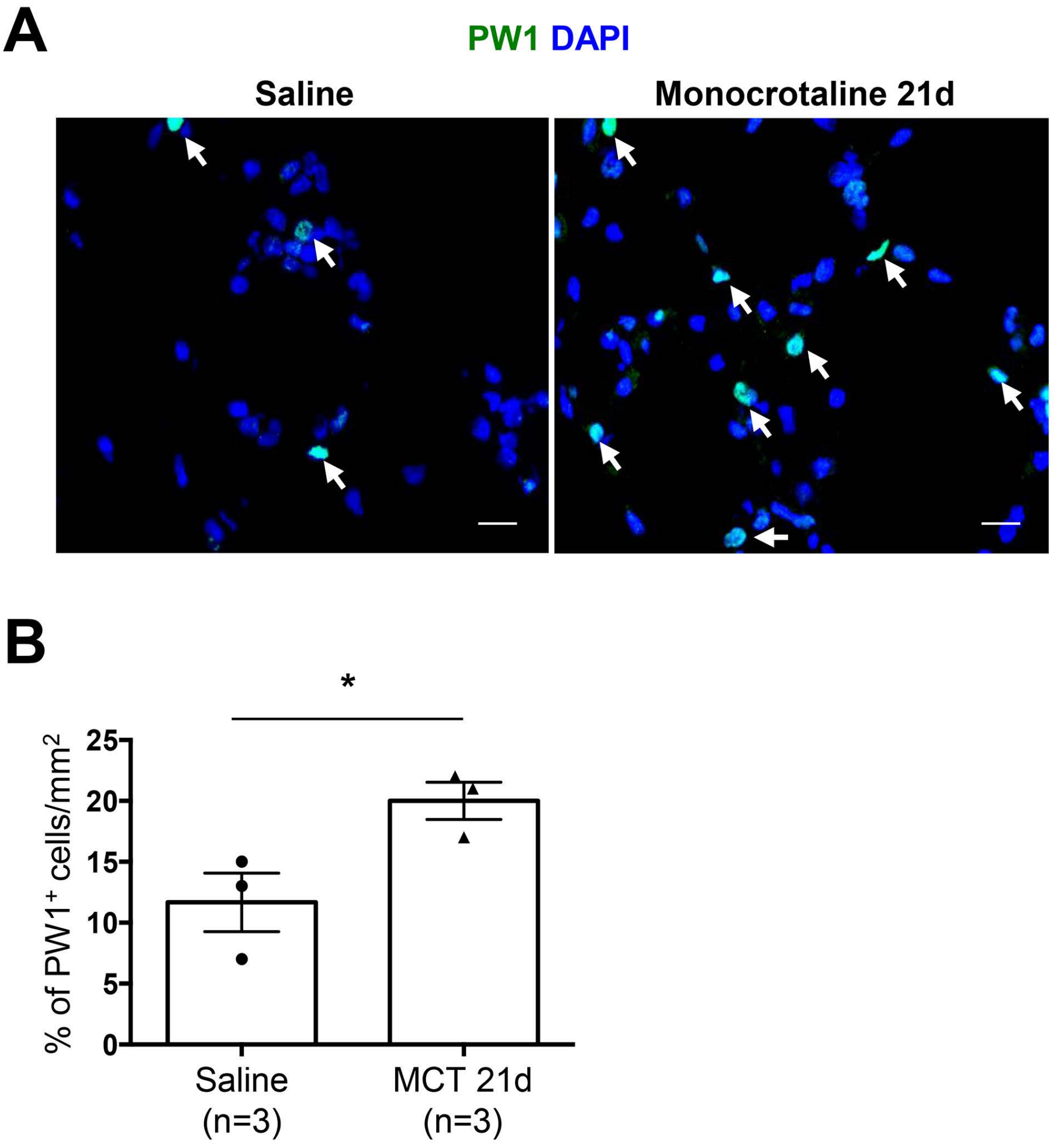
A
PW1 DAPI
Saline
Monocrotaline 21d
B
*
% of PW1+ cells/mm2
25
20
15
10
5
0
Saline
(n=3)
MCT 21d
(n=3)

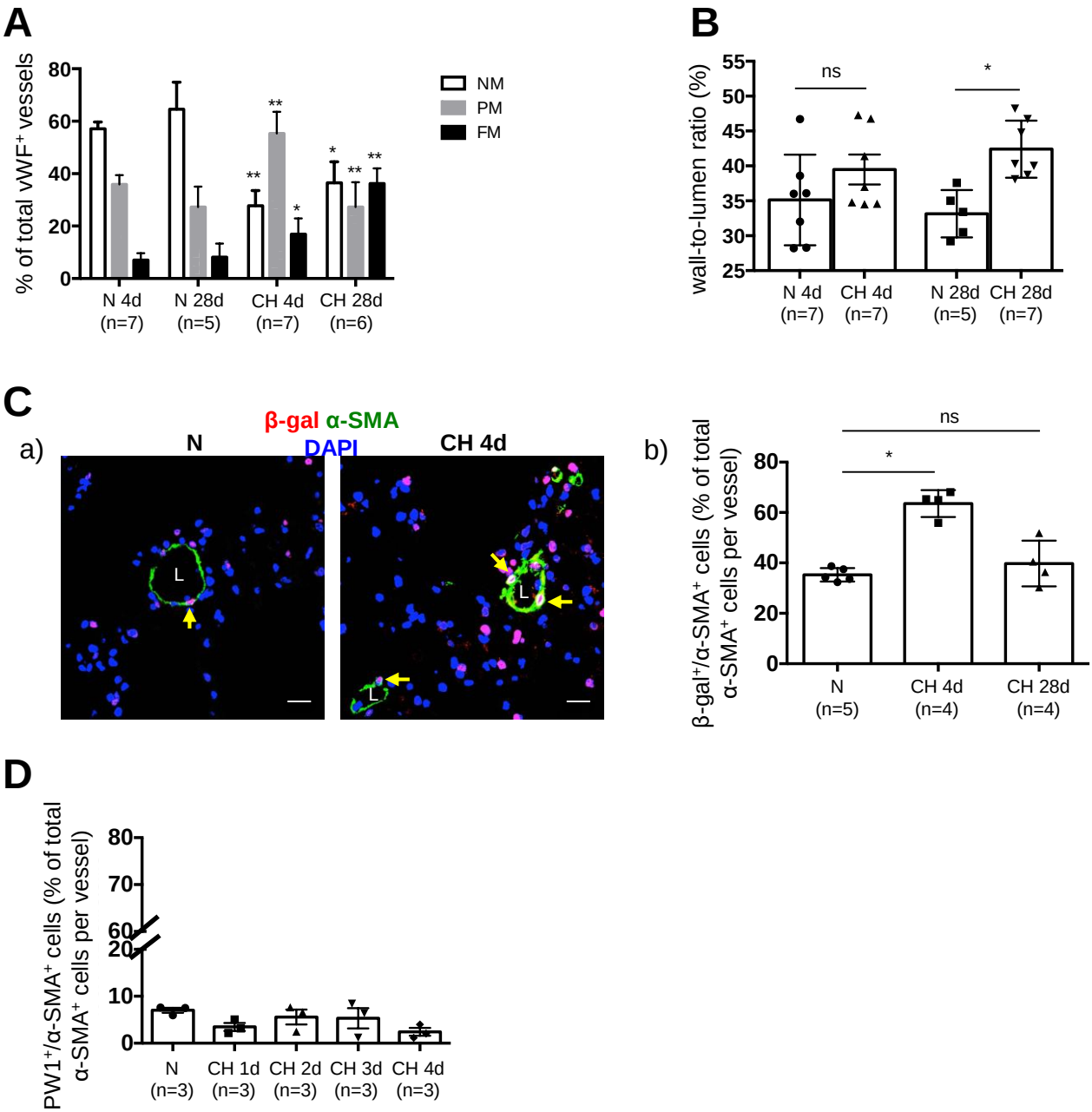
A
% of total vWF+ vessels
NM
PM
FM
N 4d (n=7)
N 28d (n=5)
CH 4d (n=7)
CH 28d (n=6)
B
wall-to-lumen ratio (%)
ns
*
N 4d (n=7)
CH 4d (n=7)
N 28d (n=5)
CH 28d (n=7)
C
a)
β-gal α-SMA DAPI
N
CH 4d
L
b)
β-gal+/α-SMA+ cells (% of total α-SMA+ cells per vessel)
ns
*
N (n=5)
CH 4d (n=4)
CH 28d (n=4)
D
PW1+/α-SMA+ cells (% of total α-SMA+ cells per vessel)
N (n=3)
CH 1d (n=3)
CH 2d (n=3)
CH 3d (n=3)
CH 4d (n=3)

Figure 5

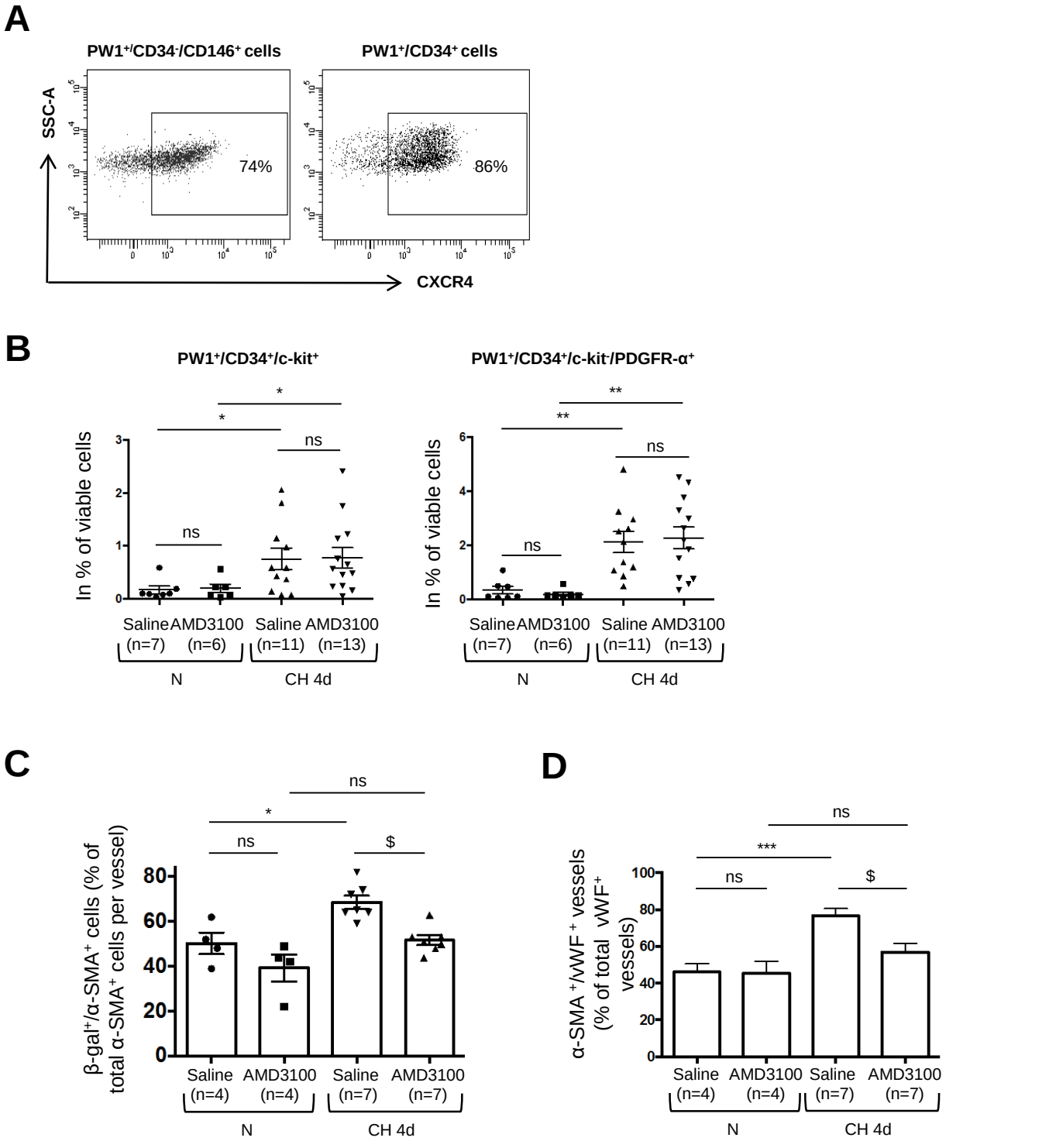
A
PW1+/CD34-/CD146+ cells
PW1+/CD34+ cells
SSC-A
74%
86%
CXCR4
B
PW1+/CD34+/c-kit+
PW1+/CD34+/c-kit-/PDGFR-α+
ln % of viable cells
ns
*
**
Saline (n=7)
AMD3100 (n=6)
Saline (n=11)
AMD3100 (n=13)
N
CH 4d
C
β-gal+/α-SMA+ cells (% of total α-SMA+ cells per vessel)
$
Saline (n=4)
AMD3100 (n=4)
Saline (n=7)
AMD3100 (n=7)
D
α-SMA+/vWF+ vessels (% of total vWF+ vessels)
***

Figure 6

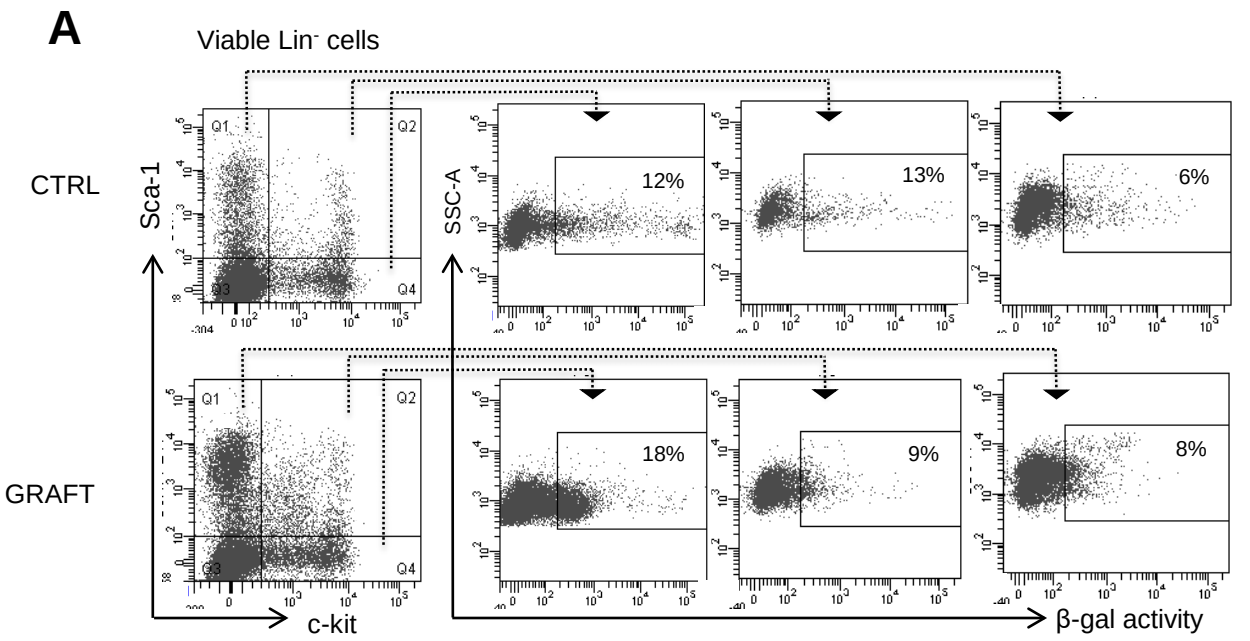
A
Viable Lin- cells
CTRL
GRAFT
Sca-1
c-kit
SSC-A
β-gal activity
Q1
Q2
Q3
Q4
12%
13%
6%
18%
9%
8%

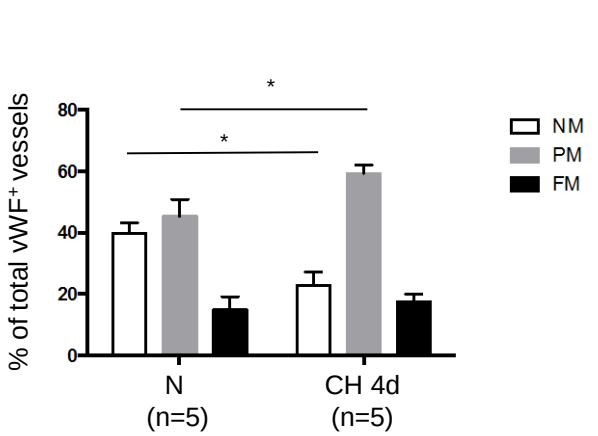
B
% of total vWF+ vessels
NM
PM
FM
N
(n=5)
CH 4d
(n=5)
*
*

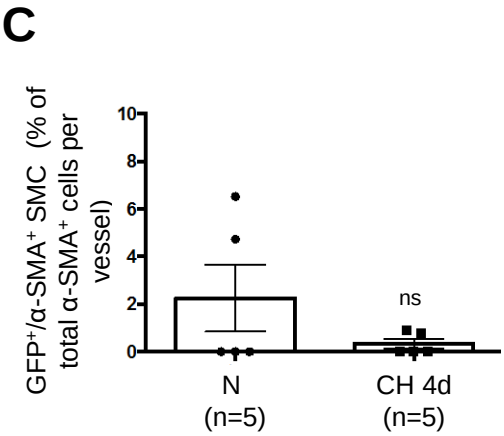
C
GFP+/α-SMA+ SMC (% of total α-SMA+ cells per vessel)
ns
N
(n=5)
CH 4d
(n=5)

Figure 7

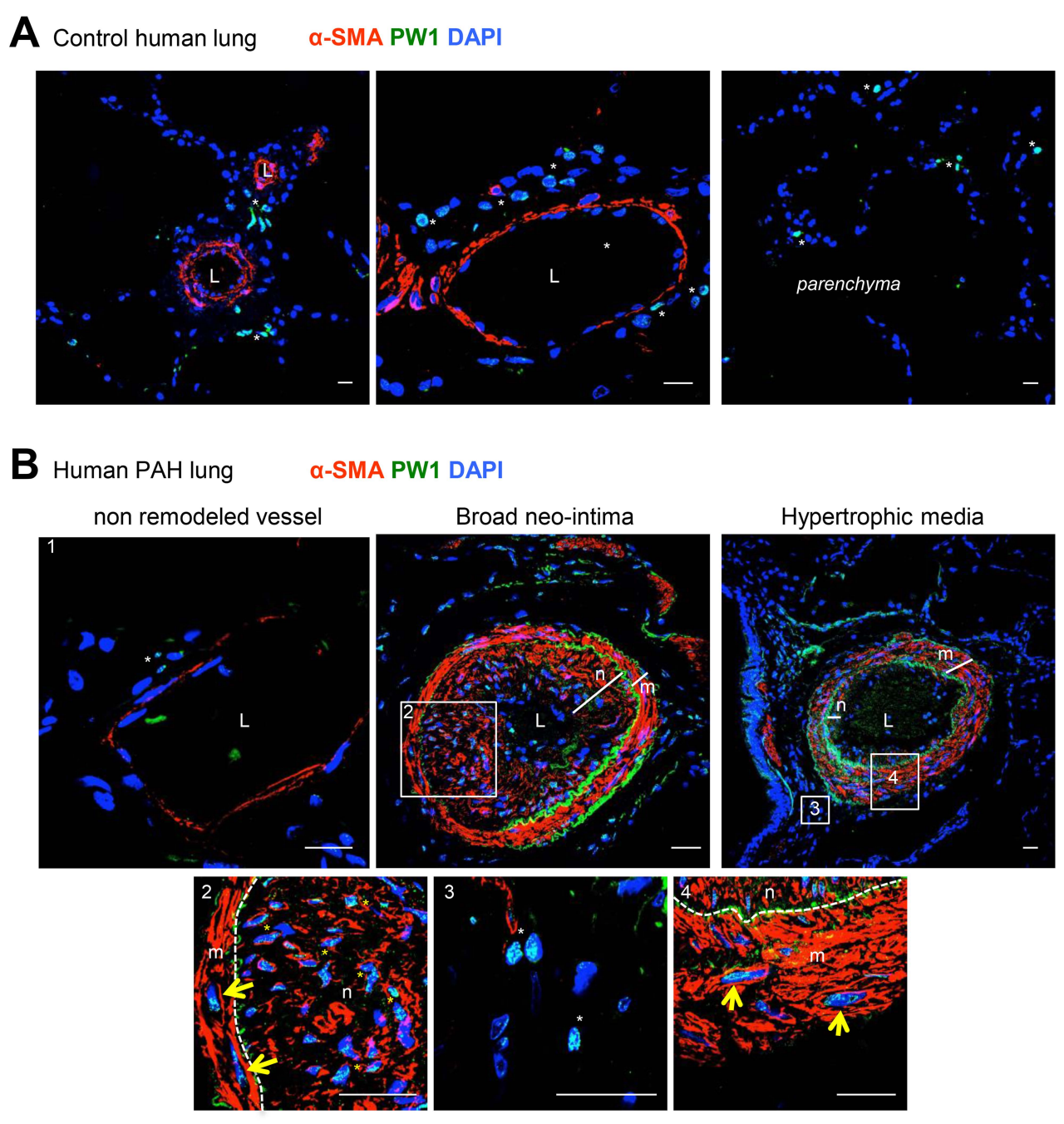
A
Control human lung
α-SMA PW1 DAPI
L
L
L
parenchyma
B
Human PAH lung
α-SMA PW1 DAPI
non remodeled vessel
Broad neo-intima
Hypertrophic media
1
L
2
L
n
m
m
n
L
4
3
2
m
n
3
4
n
m

SUPPLEMENTAL MATERIAL

Methods

Animals and experimental PAH models

Care of the animals and surgical procedures were performed according to the Directive 2010/63/EU of the European Parliament. Animals were housed in an environmentally-controlled animal facility for the duration of the experiment. All animals had access to food and water, ad libitum. *Pw1IRESnLacZ* transgenic mice (*Pw1nlacZ*/+), in which a nuclear operon lactose gene is expressed under the control of the *Pw1* gene locus were produced in our animal husbandry[1]. They were backcrossed with C57BL6/J mice and maintained in a C57BL6/J background. C57BL6/J mice were from Janvier (Orléans, France). H2B-GFP mice were originally from Jackson Labs. Mice (littermates of 6-8 weeks) were exposed to room air (normoxia) or chronic normobaric hypoxia (10% O2) in a ventilated chamber for 4 or 28 days with the same light-dark cycle. Hypoxia was obtained by flushing nitrogen into the hypoxic chamber. Levels of CO_2 and O_2 in the chamber were constantly monitored and maintained by flushing oxygen in the chamber and by absorbing CO_2 with soda lime granules. The chamber temperature was maintained at 22–24°C and excess humidity was prevented by dessicant.
Adult male Wistar rats (300 g body weight obtained from Janvier Laboratories) were injected i.p. with monocrotaline (MCT, 60 mg/kg, Fluka ref 37024) or equal volume of isotonic saline. The animals were sacrificed 3 ± 0.5 weeks later.

BrdU (5'-bromo-2'-deoxyuridine) injections

Normoxic and chronic hypoxic mice were injected i.p. with BrdU solution (Sigma, sc-290815A) prepared in PBS (100 mg/kg) at 24, 16 and 4 hours before euthanasia.

AMD3100 injections

Normoxic and chronic hypoxic mice were injected daily i.p. with AMD3100 solution (ref. A5602, Sigma-Aldrich) prepared in PBS (10mg/kg) from day 1 to day 4.

Haemodynamic measurements and tissue collection

Mice were anesthetized with a ketamine/Xylazine mix (100 and 10 mg/kg i.p.) and maintained at 37°C. After intubation, mice were connected to Minivent Mouse ventilator (type 845, Harvard Apparatus, respiratory frequency 170 stroke/min and respiratory volume 200µL). After incision of the abdomen and diaphragm, mouse right ventricular systolic pressure (RVSP) was measured by introducing a Millar pressure transducer (size 1.4 F, Millar Micro-tip catheter transducer, model SPR-671; Millar Instruments, Inc, Houston, TX, USA) into the right ventricle. Rats were anesthetized by

pentobarbital injection (50mg/kg, i.p.) and received a subcutaneous injection of METACAM (meloxicam, 1.5 mg/kg). Then, to perform RV pressure measurements, a pressure transducer catheter (size 2F, Millar model SPR-407) was advanced to the RV through the right jugular vein. The catheter was connected to a Gould amplificator to record the pressure (RS3200 Gould).

To confirm chronic hypoxia hemoglobin concentration was measured in the peripheral blood using HemoCue (Hb 20+). Right ventricular hypertrophy was assessed by calculating the weight ratio of the right ventricle (RV) to the left ventricle (LV) plus septum (S) (RV/(LV+S)).

Lungs were carefully removed and inflated by intratracheal infusion of 50% O.C.T. (Cryomatrix) in PBS, immersed in isopentane, frozen in liquid nitrogen, embedded in O.C.T and stored at -80°C. Alternatively, lungs were inflated and fixed by injecting Finefix (Milestone Srl) directly in lobes. After fixation for 24h à 4°C, lung tissues were paraffin-embedded.

FACS analysis

Lung single-cell suspensions were obtained by digestion the tissues in DMEM high glucose media (Gibco) supplemented with 20% FBS and 0.5 mg/mL of collagenases IA-S, II-S, IV-S (Sigma) for 45 min at 37°C. The remaining tissue fragments were next disrupted by mechanically between two super-frost+ slides (Thermo Scientific), to separate the progenitor cells from the extracellular matrix[2]. Bone marrow was prepared by flushing bones with DMEM. Mice lung cells or bone marrow preparation were stained for 20 min on ice in the dark. Antibodies used were CD45 PECy7, CD34 Brilliant Violet 421, PDGFR-α PE, CD146 PE, c-kit PE or APC, CXCR4 PE, Lin Pacific Blue cocktail (see Online Table II). To detect nuclear β-gal activity, two different substrates were optimized and used: FDG kit for bone marrow cells or DDAO-G kit for lung cells (both from Life Technologies). β-gal$^+$ cells were defined as having a signal higher as compared to the cells isolated from non-transgenic mouse (β-gal$^-$). 7-AAD (BD Pharmigen) for bone marrow cells and Live dead blue dye (Life Technologies) for lung cells were used as viability cell marker. Cells were sorted using FACSAria (Becton Dickinson) with appropriate isotype matching controls and the Fluorescence Minus One controls (FMO) were used to identify and gate cells.

Primary cell culture – Differentiation induction

Immediately after sorting, isolated cells were plated on matrigel-coated (ref. 354277, Life Sciences-Corning) dishes for smooth muscle and endothelial cell differentiation, or gelatin-coated (Attachement Factor protein, ref. S-006-100, ThermoFisher) dishes for skeletal muscle cell differentiation.

For smooth muscle cell differentiation, isolated cells were plated at a density of 2000 cells/cm^2 and were grown for three days in DMEM 20% FBS (Sigma), 2% (v/v) penicillin-streptomycin (Gibco) then cells were transferred in DMEM 2% FBS, 1% (v/v) penicillin-streptomycin, supplemented with TGF-β_1 (2 ng/mL) (ref. 7666-MB-005, R&D systems) and PDGF-BB (20 ng/mL) (ref. 220-BB-010, R&D systems) for 10 days, this medium was changed every 2 days.

For skeletal muscle cell differentiation, isolated cells were plated at a density of 2000 cells/cm^2 and were grown for three days in DMEM supplemented with 2.5 ng/mL basic fibroblasts growth factor (bFGF, ref. 233-FB-025, R&D systems), 20% FBS (Sigma), 10% heat-inactivated horse serum (Gibco), 1% (v/v) penicillin-streptomycin (Gibco), 1% (v/v) L-glutamine (Gibco) and 1% (v/v) sodium pyruvate (Gibco). This growth medium was changes every 2 days. Then cells were transferred in DMEM 5% heat-inactivated horse serum and 1% (v/v) penicillin-streptomycin, for 2 days.
For endothelial cell differentiation, isolated cells were plated at a density of 5000 cells/cm^2 and were grown for 10 days in complete EGM-2 (Endothelial growth medium, Lonza) supplemented with 20 ng/mL $VEGF_{164}$ (ref. 493-MV-005, R&D systems) and 1% (v/v) penicillin-streptomycin. This medium was changed every 2 days.

Immunofluorescent labeling

Tissue 10µm thick cryosections were fixed in formalin (Sigma). Tissue paraffin-embedded 4µm thick sections were deparaffinised, rehydrated, and citrate antigen retrieval was performed. Sorted cells were centrifuged in 150 µL PBS onto a gelatin-coated slide using a Cytospin 3 cytocentrifuge (Shandon Instruments, PA) and were fixed in formalin (Sigma). Then cryosections and cytospun cells were permeabilized in methanol (6 min at -20°C) or with X-100 triton 0.01% in PBS (5 min at RT). Non specific binding was blocked with bovine serum albumin 10% in PBS (1h at RT) and sections were incubated overnight with PBS + primary Abs (see Online Table III) at 4°C. Secondary Abs and DAPI (DAPI) were diluted in PBS (respectively 1/500 and 1/1000) and incubated 45 min at RT. Immunolabeled sections were mounted with Dako fluorescent mounting medium (Dako) and examined under confocal microscope (Leica SPE confocal microscope). In some cases, as indicated, images were acquired with a cooled CoolSnap camera (Roper-Scientific) on an Olympus epifluorescent microscope (60x, UPlanSApo, 0.17). Images were processed and analyzed using Metamorph software (Molecular Devices) supplemented with the 3D-deconvolution module. For each sample, a series of consecutive planes (stack of images) were acquired (sectioning step, 0.2 µm) and deconvoluted using acquired point spread function. Control experiments were performed using secondary antibodies alone and showed no non-specific labeling.

Quantitative analysis by immunofluorescent microscopy

Images were analyzed by an investigator blinded to the experimental status of all animals. β-gal$^+$ and β-gal$^-$/α-SMA$^+$ SMC were counted for all fully muscularized vessels (<100 µm) of one lung section per animal (15-30 vessels/animal) using stacks of 5-10 consecutive planes for one image to ensure co-localization of the nuclear labeling of β-gal and the cytoplasmic labeling of α-SMA. For other countings, single planes were analyzed for each image and a minimum of 30 to 60 fields were analyzed per animal.

Muscularization was measured by immunofluorescence in using using anti-α-SMA and anti-vWF antibodies. Vessels showing a perimeter with more than 90% of muscularization were considered fully muscularized. Medial thickness was measured as wall-to-lumen ratio.

Bone marrow transplantation

20 female 8 weeks-old C57BL6/J mice were subjected to 2x6 Gy (7.2 min; 0.83 Gy/min) lethal total body irradiation within 24h. Immediately after the second irradiation, isoflurane-anesthetized mice were reconstituted by direct intravenous injection (in retro-orbital plexus) with 10.10^6 cells in PBS freshly isolated from bone marrow of age and sex-matched $GFP^+/\beta\text{-gal}^+$ (H2B-GFPx*Pw1*$^{nLacz/+}$) or $\beta\text{-gal}^+$ (*Pw1*$^{nLacz/+}$) mice (both on C57BL6/J background). This latter was performed to confirm the good reconstitution of the $PW1^+/\beta\text{-gal}^+$ populations in the grafted mice's bone marrow by FACS analysis using the FDG substrate. Reconstitution of the $PW1^+/\beta\text{-gal}^+$ niche was found to be complete 6 months after transplantation. At this time, the percentage of $GFP^+/CD45^+$ cells in blood mononuclear cells of $GFP^+/\beta\text{-gal}^+$ grafted mice was measured by FACS (LSRFortessa, Becton Dickinson), to confirm the total bone marrow reconstitution. These mice were then exposed to normoxia or chronic hypoxia for 4 days.

Statistical analysis

All values were expressed as the mean ± SEM. Statistics were performed using the computer program GraphPad PRISM 6 (GraphPad software) or XLStat 2013 (Addinsoft, New York, USA) with a non-parametric Mann and Whitney test for single comparisons. Multiple comparisons were analyzed using Kruskall-Wallis test followed by Dunn post-hoc test. P values less than 0.05 were considered to be significant.

Study approval

Experiments for the project were approved by our institutional review board (authorizations Ce5/2012/023 and Ce5/2012/050).

Study patients were part of the French Network on Pulmonary Hypertension, a program approved by our institutional Ethics Committee (Protocol N8CO–08–003, ID RCB: 2008-A00485-50, approved on June 18, 2008). Written informed consent was received from participants prior to inclusion in the study.

References

1. Besson V, Smeriglio P, Wegener A, Relaix F, Nait Oumesmar B, Sassoon DA, Marazzi G. PW1 gene/paternally expressed gene 3 (PW1/Peg3) identifies multiple adult stem and progenitor cell populations. *Proc Natl Acad Sci U A* 2011;108:11470-5.

2. Crisan M, Huard J, Zheng B, Sun B, Yap S, Logar A, Giacobino J-P, Casteilla L, Péault B. Purification and culture of human blood vessel-associated progenitor cells. *Curr. Protoc. Stem Cell Biol.* 2008;Chapter 2:Unit 2B.2.1-2B.2.13.

SUPPLEMENTAL FIGURES

Online Figure I

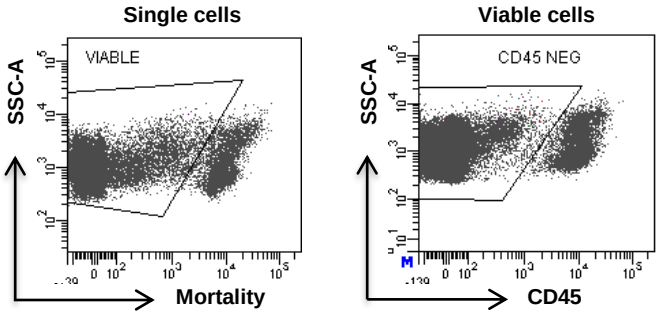

Online Figure I: Representative FACS profile of total mouse lung cells indicating the gating strategy to sort the three PW1^{+} populations with Live dead blue dye (viability marker) and CD45 antibody. Viable CD45^{-} cells were then separated by CD34, c-kit, and DDAO expression as shown in Figure 1B.

Online Figure II

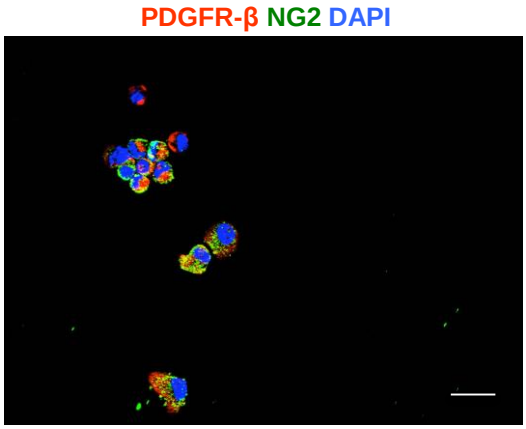

Online Figure II: Expression of other pericyte markers. PDGFR-β (red) and NG2 (green) were also analysed by immunofluorescence in the PW1^{+}/CD34^{-}/CD146^{+} population. Representative image (n=2). Epifluorescence microscopy. Scale bars: 20µm.

Online Figure III

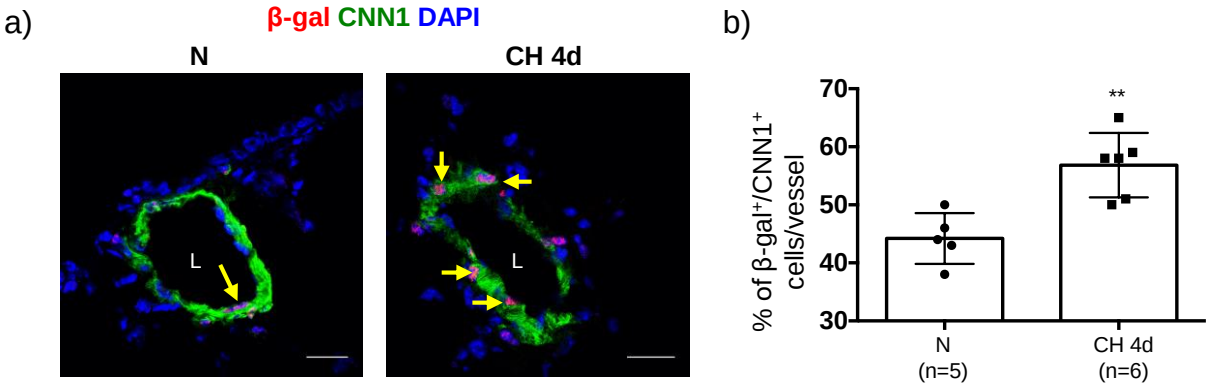

Online Figure III: Chronic hypoxia-induced neomuscularization is associated with an increased number of PW1^{+}-derived β-gal^{+}/CNN1^{+} SMC. Quantification of lung β-gal-expressing SMC in normoxic and chronic hypoxic 4 days mice (CH 4d). a) Representative images of lungs from N or CH 4d mice, stained with b-galactosidase (red) and CNN1 (green). b) The percentage of lung β-gal^{+}/CNN1^{+} cells (yellow arrowheads) in muscularized vessels (<100 µm) was determined by immunofluorescence from normoxic (n=5), and CH 4 days (n=6) mice. The number of b-gal-expressing SMC was significantly increased after 4 days of CH. L: Lumen. Confocal microscopy. Scale bars: 20µm. Values are means ± SEM, ** p<0.01 versus N (two-tailed MW).

Online Figure IV

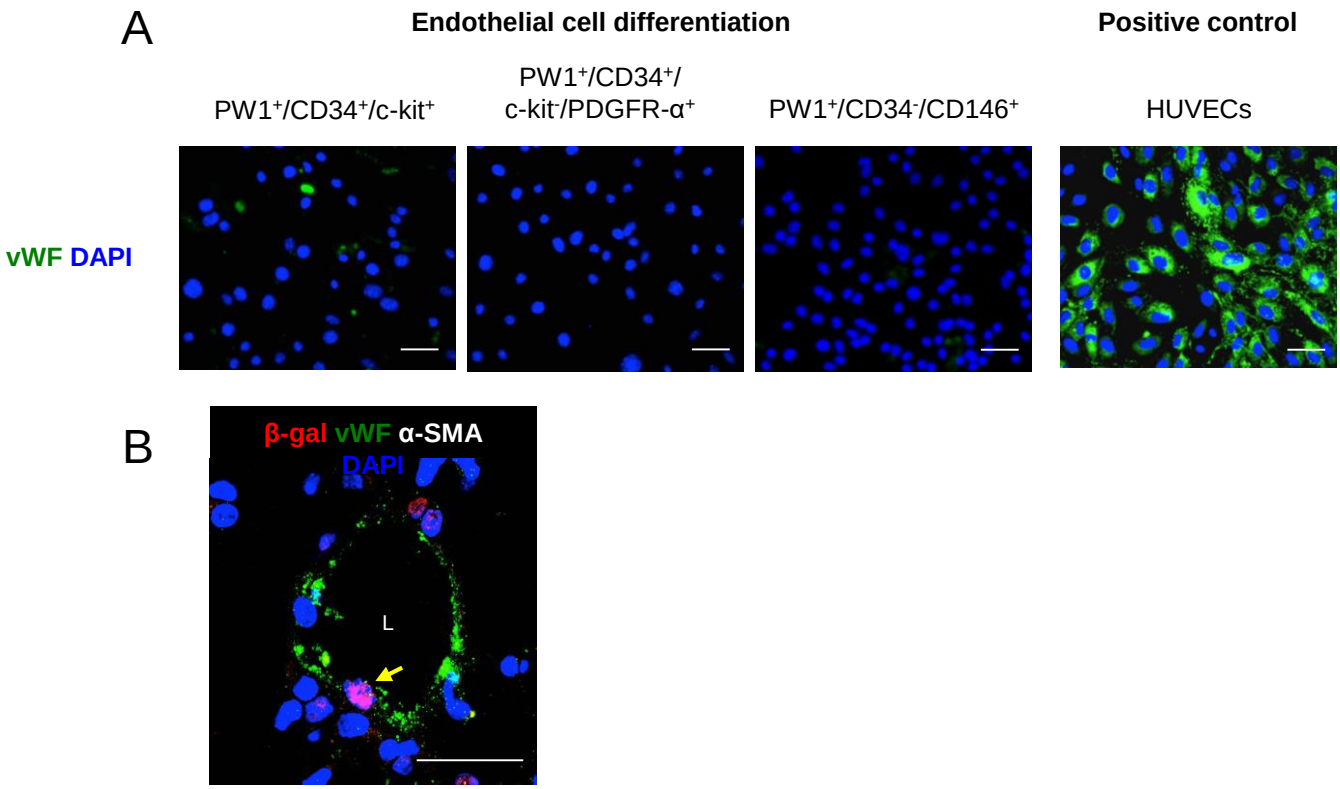

Online Figure IV **:** The mouse lung PW1$^+$ cells do not differentiate into endothelial cell (EC). **(A)** FACS isolated PW1$^+$ cell populations were grown in EGM-2 supplemented with VEGF and immunostained after culture for EC marker vWF (green) show no staining. HUVECs were used as positive control. Representative images of multiple experiments (n=2). **(C)** Mouse lungs immunostained for β-gal (red) and for EC marker vWF (green) show one of the rare EC expressing β-gal in the intima of pulmonary vessels (yellow arrowhead). Confocal microscopy. L: Lumen of vessel. Scale bars: 20μm.

Online Figure V

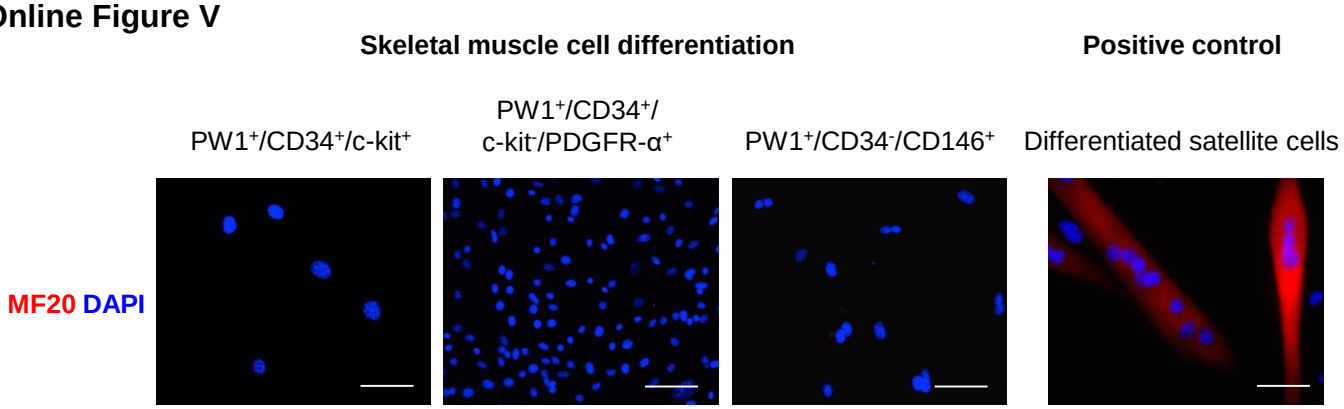

Online Figure V **:** The mouse lung PW1$^+$ cells do not differentiate into skeletal muscle cells. FACS isolated PW1$^+$ cell populations were grown in myogenic conditions and immunostained for skeletal muscle cell marker, skeletal myosin heavy chain, MF20 (red) show no staining. Differentiated satellite cells were used as positive control. Representative images of multiple experiments (n=2). Epifluorescence microscopy. Scale bars: 20μm.

Online Figure VI

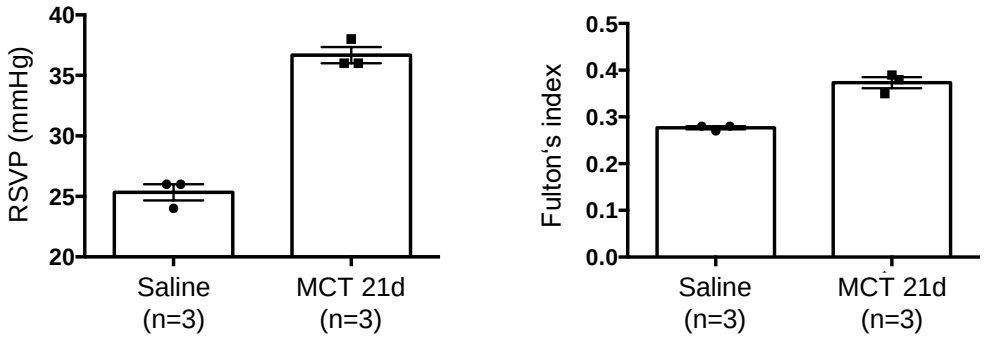

Online Figure VI: Monocrotaline (MCT) induces the increase of the right systolic ventricular pressure (RVSP, in mmHg) and the elevation of the fulton's index 21 days after the single MCT-injection (Ratio of RV to LV plus septum weight, RV/LV+S) in rats. Values are means ± SEM.

Online Figure VII

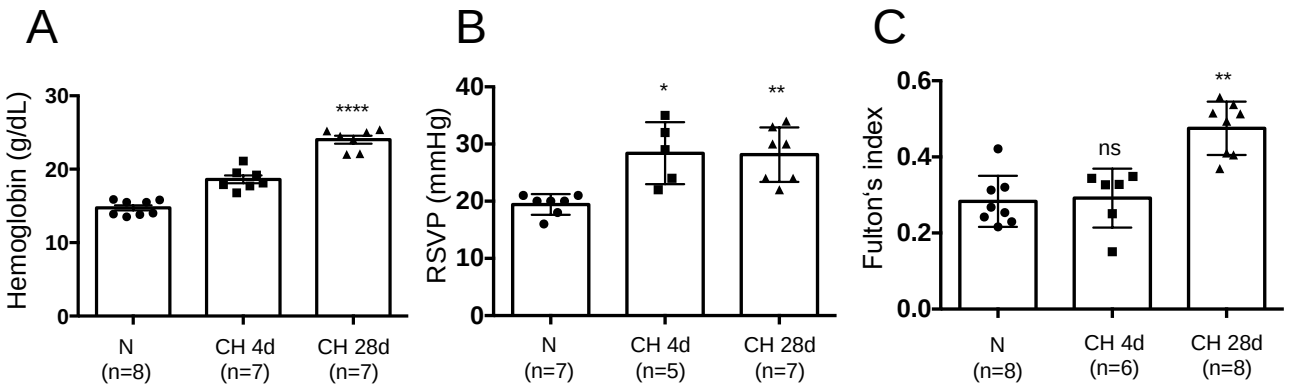

Online Figure VII: Chronic hypoxia (CH) induces **(A)** the increase of the hemoglobin concentration (g/dL) in peripheral blood, **(B)** the elevation of the right systolic ventricular pressure (RVSP, in mmHg) and **(C)** the elevation of the fulton's index after 28 days of CH (Ratio of RV to LV plus septum weight, RV/LV+S) in mice. Values are means ± SEM, * p<0.05, **p<0,01, ****p<0,0001 vs N (normoxia) (KW-Dunn).

Online Figure VIII

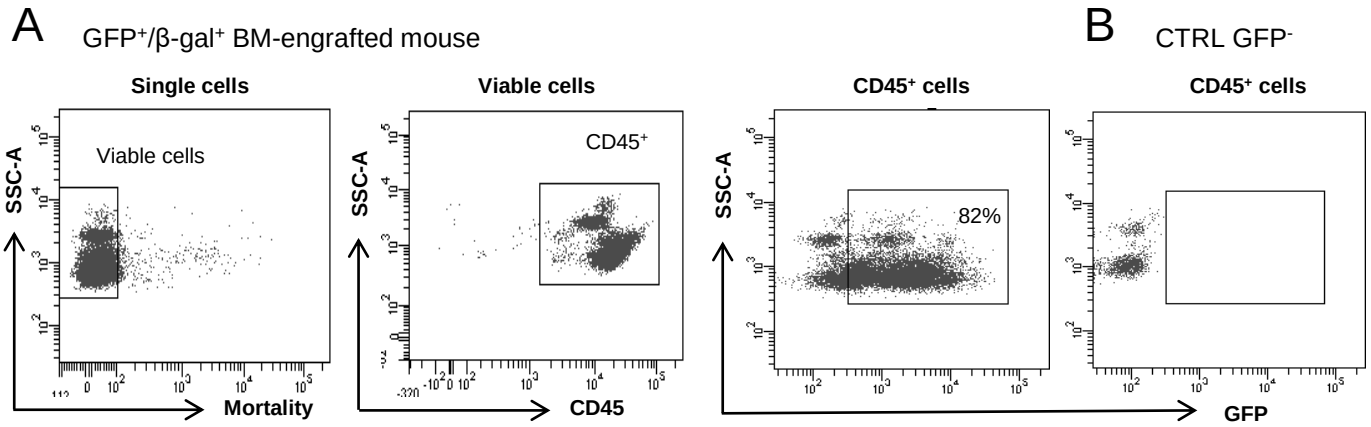

Online Figure VIII: Flow cytometry analysis of peripheral blood cells from **(A)** GFP^+ BM-transplanted mouse 6 months after transplantation and **(B)** control GFP^- mouse. Viable $CD45^+$ cells were analyzed for GFP fluorescence. The transplanted mice showed a good chimerism (82,2±4,2%). Representative image of BM-engrafted mice (n=10). The percentage is indicated in percentage of viable $CD45^-$ cells.

SUPPLEMENTAL TABLES

Online Table I

PAH patients	gender	age (yrs)	BMPR2 mutation	PAP (mmHg)	CI (L/min/m^2)	PVR (Wood units)	NYHA	Therapy
1	Female	31	No	61	1,6	14	III	IV prostacyclin+ERA+ PDE5-i
2	Male	50	No	43	3,23	5,61	III	IV prostacyclin+ERA
3	Female	38	No	43	2,2	8,16	III	IV prostacyclin+ERA+ PDE5-i

Control patients	gender	age (yrs)	Disease
1	Female	36	pulmonary adenocarcinoma
2	Female	51	pulmonary adenocarcinoma
3	Female	47	pulmonary adenocarcinoma

Online Table I: Clinical characteristics of patients in the study. PAP = pulmonary arterial pressure. CI = cardiac index. PVR = pulmonary vascular resistance. NYHA = New York Heart Association. IV prostacyclin = intravenous prostacyclin. ERA = endothelin receptor antagonist. PDE5-I = phosphodiesterase type 5 inhibitor.

Online Table II

Abs	Ref	Company
CD45 PECy7	25-0451-82	eBioscience
CD34 BV421	119321	Biolegend
PDGFR-α FITC	11-1401-82	eBioscience
CD146 PE	134704	Biolegend
c-kit APC	17-1172	eBioscience
c-kit PE	135105	Biolegend
Lin Pacific blue	88-7772-72	eBioscience
Sca-1 PE	12-5981-82	eBioscience
CXCR4 PE	551966	BD

Online Table II: FACS antibodies, references and companies are indicated.

Online Table III

Abs	Ref	Company	Dilution	Incubation time
PW1	Relaix et al, 1996	-	1/2000	OVN, 4°C
PEG3	ABIN 735653	Antibodies online	1/200	OVN, 4°C
β-galactosidase	ab9361	Abcam	1/6000	OVN, 4°C
vWF	ab11713	Abcam	1/300	1h30, RT (OCT sections)
vWF	ab9378	Abcam	1/100	OVN, 4°C (cell)
vWF	11778-1-AP	proteintech	1/50	OVN, 4°C (paraffin sections)
FITC α-SMA	F3777	Sigma	1/500	1h30, RT
α-SMA	M0851	Dakocytomation	1/300	1h30, RT
CNN1	ab466794	Abcam	1/300	1h30, RT
SM-MHC	ab53219	Abcam	1/100	OVN, 4°C
MF20	AB 2147781	Developmental Studies Hybridoma Bank	1/50	OVN, 4°C
c-kit	ab25022	Abcam	1/100	1h30, RT
PDGFR-α	BD558774	BD	1/500	1h30, RT
CD146	134701	Biolegend	1/2000	1h30, RT
NG2	AB5320	Millipore	1/500	OVN, 4°C
PDGFR-β	14-1402-82	eBioscience	1/2000	OVN, 4°C
BrdU	ab6326	Abcam	1/500	OVN, 4°C
GFP	TP401	Torres Pines Biolabs	1/300	OVN, 4°C

Online Table III: Antibodies used for immunofluorescence, references, companies, appropriate dilutions and incubation conditions are indicated. RT, room temperature; OVN, overnight.